Electronic Supplementary Material (ESI) for ChemComm.

Hybrid Uranyl-Vanadium Nano-Wheels

Ganna A. Senchyk[†], Ernest M. Wylie[†], Sarah Prizio[†], Jennifer E.S. Szymanowski[†] Ginger E. Sigmon[†], and Peter C. Burns*[,†,‡]

[†]Department of Civil & Environmental Engineering & Earth Sciences, University of Notre Dame, Notre Dame, Indiana 46556, United States

[‡]Department of Chemistry & Biochemistry, University of Notre Dame, Notre Dame, Indiana 46556, United States

SUPPORTING INFORMATION

Synthesis

Caution: Although depleted uranium was used in these experiments, it is radioactive and should only be handled by qualified personnel in appropriate facilities.

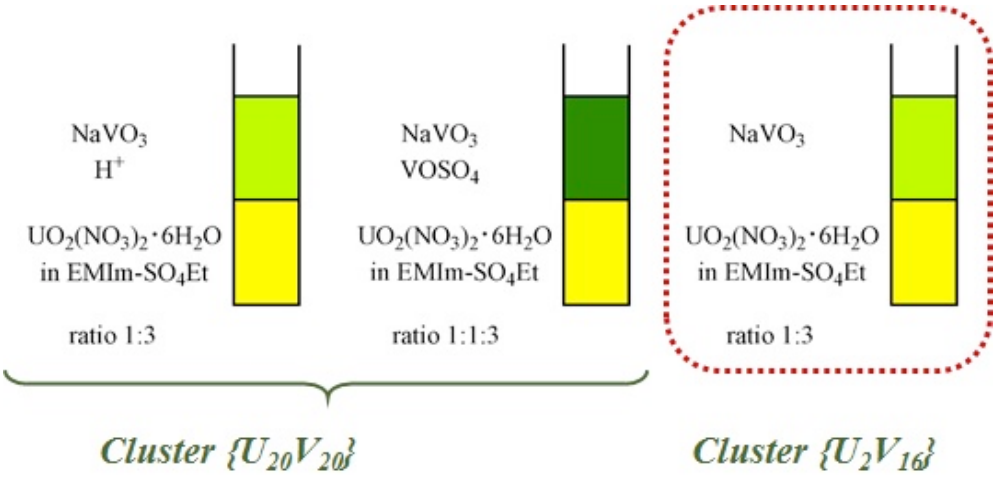

***{U20V20}*, *(EMIm)15Na5[(UO2)20(V2O7)10(SO4)10]·80H2O* (1a).**

Compound **1a** was first synthesized by dissolving uranyl nitrate (24.8 mg) into 0.5 mL 1-ethyl-3methylimidazolium (>95%) in a 5 mL vial and layering a 0.5 mL aqueous solution containing $NaVO_3$ (18.5 mg) above the ionic liquid phase. Over the course of several months, large, yellow-green crystals of **1a** were observed at the surface of the mixture as well as at the interface between the two phases.

Subsequently, **1a** was obtained by carefully layering 0.5 mL of $NaVO_3$ 0.3 M aqueous solution with 0.02 mL of H_2SO_4 (1M) over 0.5 mL of $UO_2(NO_3)_2$ 0.1 M solution in EMIm-SO_4Et ionic liquid (ratio of components V^{5+}:U^{6+} is 3:1). A yellow-orange precipitate immediately formed on the boundary between the liquid phases, and subsequently the solution turned from orange to light green, and within one month light green prisms appeared on the top of the solution (yield after two months ~ 10% based on U).

Increasing the concentration of acid leads to formation of orange crystals of decavanadate $\{V_{10}\}$ polyoxoanions in a mixture with **1a**.

Compound **1a** was also obtained by carefully layering 0.5 mL of $NaVO_3$ 0.3M water solution and 0.5 mL of $VOSO_4$ 0.1 M water solution over 0.5 mL of $UO_2(NO_3)_2$ 0.1 M solution in EMIm-SO_4Et ionic liquid (ratio of components V^{5+}:V^{4+}:U^{6+} is 3:1:1). A green precipitate immediately formed on the boundary between the phases and the solution changed color to green. Light green prisms suitable for single crystal X-ray diffraction appeared within two weeks (yield in one month reaches 10% based on U).

Other ratios of V^{5+}:V^{4+}:U^{6+} also gave compound **1a**, but in mixtures with unknown small dark-green crystals that are X-ray amorphous.

{U_2V_{16}}, $(EMIm)_8[(UO_2)_2(V_{16}O_{46})]\cdot 4H_2O$ (**2**). 0.5 mL of $NaVO_3$ 0.3 M water solution was carefully layered on 0.5 mL of $UO_2(NO_3)_2$ 0.1 M solution in EMIm-SO_4Et ionic liquid (ratio of component V^{5+}:U^{6+} is 3:1). A yellow precipitate immediately formed at the boundary between phases and in one week a mixture of green rhombic crystals of **2** appear in this precipitate (total yield ~ 10% based on U).

A broad synthetic screening with V^{5+}:U^{6+} ratio variation indicated that lower V^{5+} concentrations (one and two equivalents) can give the desired products, but with slower reaction times and lower yield, while higher concentrations of V^{5+} (more than 4 equivalents) give a mixture of green crystals of *{U_2V_{16}}* and orange crystals of decavanadate {V_{10}} polyoxoanions.

In order to optimize the synthetic procedure and the yield of pure crystals of **1a** and **2**, we found that liquid-liquid layering was not necessary. Using the same reactants as described above, we mixed solutions and stirred them for 30 minutes, following by removal of an amorphous precipitate by filtration. These precipitates were analyzed by X-ray diffraction, but they remain unidentified (see results below). In two days (for **2**) or in two weeks (for **1a**) crystals started to appear from the solutions. In some cases the reaction mixture for compound *{$U_{20}V_{20}$}* crystallizes light green crystals with other unit cell $(EMIm)_{15}Na_5[(UO_2)_{20}(V_2O_7)_{10}(SO_4)_{10}]\cdot nH_2O$ (**1b**) that contains the *{$U_{20}V_{20}$}* clusters in a different packing arrangement. Two slightly different packing modes are observed for *{U_2V_{16}}* clusters as well that always form together (see PXRD below), but the second crystals are twinned and it was impossible to fully resolve the structure.

Synthesis reactions were conducted that were similar to those described above but that used different ionic liquids containing Imidazolium cations (bistriflimide or diethyl phosphate anions), but did not yield either **1** or **2**.

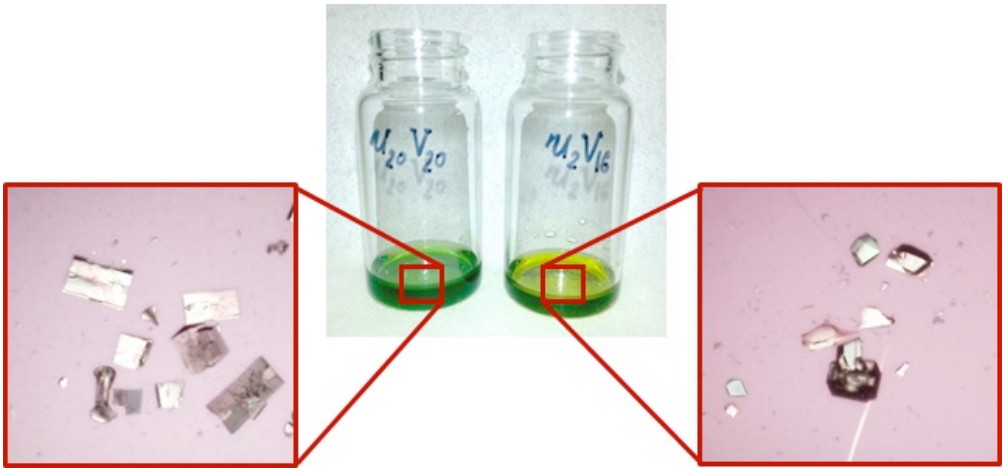

Elemental analysis

Crystals were separated from their mother solutions by vacuum filtration through Whatman1 filter membranes and rinsed with methanol. About 10 mg of each sample were recovered and dissolved in 5% HNO_3, and these solutions were analyzed using a Perkin-Elmer inductively coupled plasma optical emission spectrometer (ICP-OES). For CHN, crystals were analyzed using a Costech elemental analyzer (ECS 4010).

Table S1. Results of elemental analysis for **1a,1b** and **2** and precipitates filtered from reaction mixtures.

	{$U_{20}V_{20}$} (1a)		**{$U_{20}V_{20}$} (1b)**		**{U_2V_{16}} (2)**		**$U_{20}V_{20}$_prec**	**U_2V_{16}_prec**
	Calc.	*Found*	*Calc.*	*Found*	*Calc.*	*Found*	*Found*	*Found*
C	9.08%	9.01%	10.30%	10.26%	19.00%	19.10%	24.50%	25.31%
H	2.92%	2.83%	1.81%	1.72%	3.12%	3.20%	4.30%	4.43%
N	3.53%	3.55%	4.00%	4.10%	7.39%	7.33%	8.04%	8.22%
U	39.99%	39.26%	45.34%	45.02%	15.69%	15.15%	13.20%	16.20%
V	8.56%	8.69%	9.70%	9.79%	26.86%	26.27%	11.09%	11.23%
S	2.69%	2.73%	3.03%	2.89%	-	-	7.32%	7.51%
Na	0.97%	0.96%	1.09%	1.05%	-	-	0.24%	0.31%

Elemental analysis yielded a general formula for the X-ray amorphous:
$U_{5.3}V_{20.8}S_{22}Na_1O_{187.5}N_{55}C_{195.6}H_{195.6}$ – from the *$U_{20}V_{20}$*-reaction, and
$U_5V_{16.3}S_{17.4}Na_1O_{124.2}N_{43.6}C_{156.6}H_{328.7}$ – from the *U_2V_{16}*-reaction. These formulas do not correspond to **1a,1b** (*{$U_{20}V_{20}$}* crystals) or **2** (*{U_2V_{16}}* crystals), and are likely due to mixtures of several compounds.

Powder XRD

PXRD spectra were measured for powders using a Bruker D8 ADVANCE.

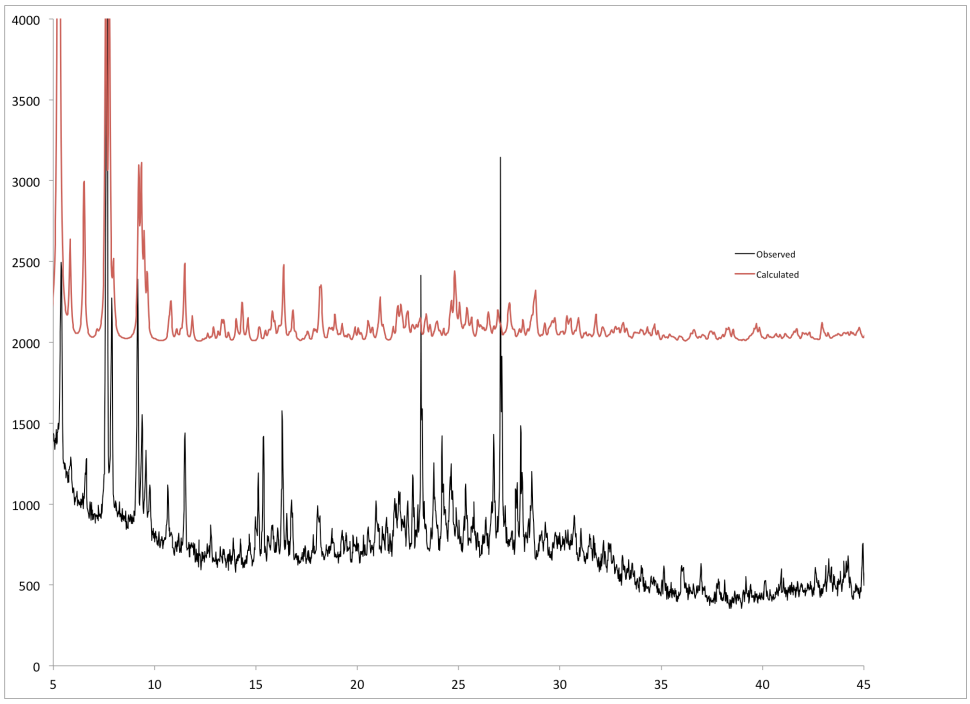

Figure S1. Simulated and experimental PXRD patterns of compound **1a**. Crystals of U20V20 became mostly X-ray amorphous upon grinding, although they diffract well as single crystals. As such, we gathered together as many crystals as possible, and very lightly crushed them prior to collection of the powder diffraction pattern. Even with this modest grinding, a significant amorphous component is introduced, as shown by the background of the diffraction pattern shown in Fig. S1. Also, the intensities of the diffraction lines are not reliable relative to those for a fine powder with random orientations of crystallites. The relatively thick "powder" caused a small offset of the diffraction pattern, which has been corrected here.

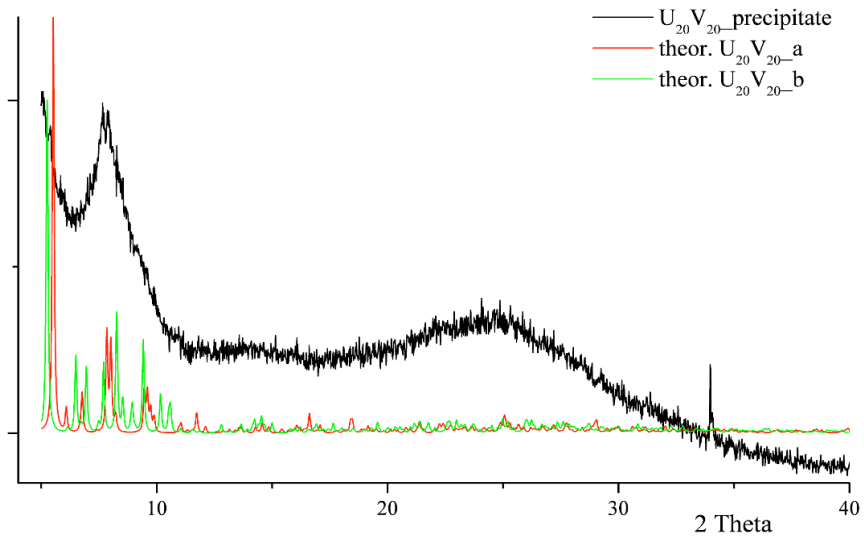

Figure S2. PXRD pattern of precipitate from $U_{20}V_{20}$-reaction, and simulated patterns of compounds **1a** and **1b**. The precipitate is mostly amorphous with small quantity of unidentified crystalline component.

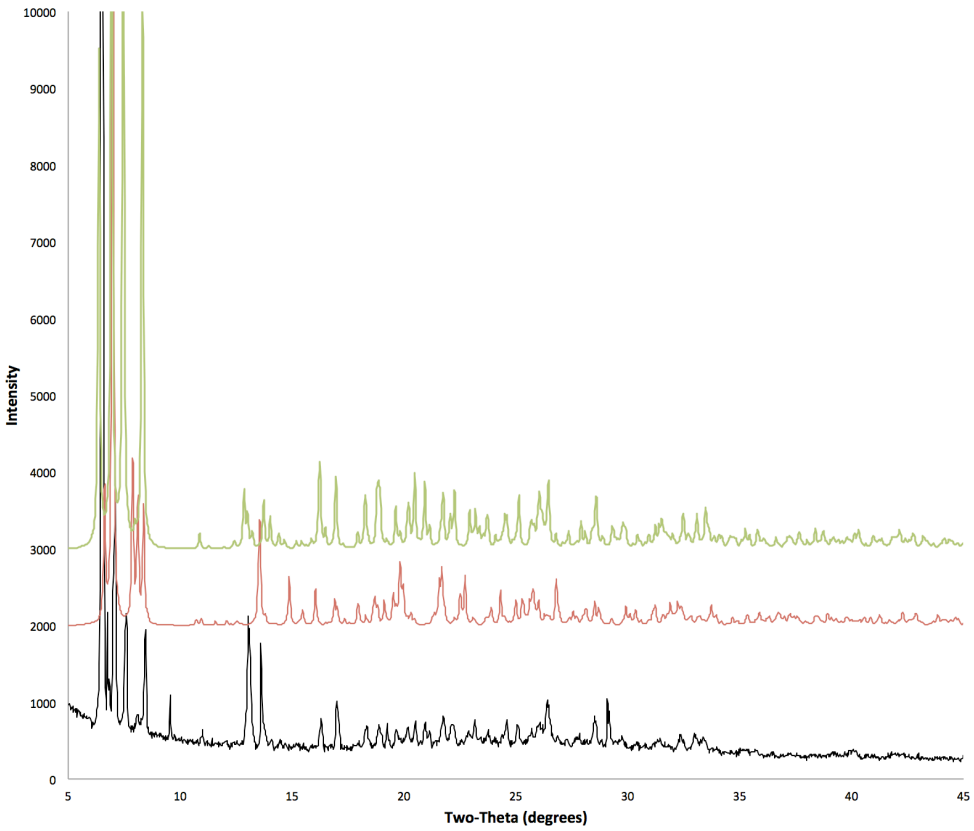

Figure S3. Experimental PXRD pattern of *{U_2V_{16}}* crystals and simulated pattern from single-crystal data of compound **2** and its isomorphous modification. Crystals became mostly X-ray amorphous upon grinding, although they diffract well as single crystals. As such, we gathered together as many crystals as possible, and very lightly crushed them prior to collection of the powder diffraction pattern. Even with this modest grinding, a significant amorphous component is introduced, as shown by the background of the diffraction pattern shown in Fig. S1. Also, the intensities of the diffraction lines are not reliable relative to those for a fine powder with random orientations of crystallites. The relatively thick "powder" caused a small offset of the diffraction pattern, which has been corrected here.

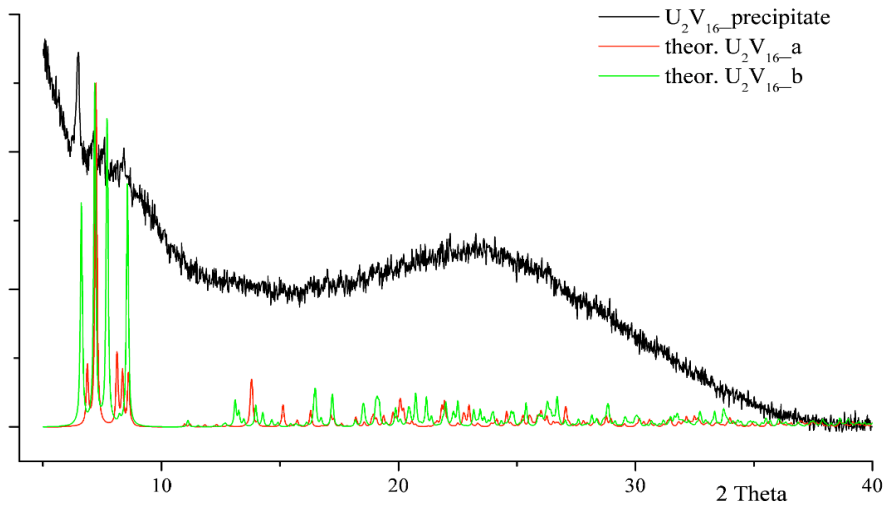

Figure S4. PXRD pattern of solid precipitate from the U_2V_{16}-reaction, and simulated patterns of compounds **2** and its isomorphous modification. The precipitate is mostly amorphous with a small quantity of crystalline U_2V_{16}-component.

IR spectroscopy

Infrared spectra were collected from single crystals using a SensIR technology IlluminatIR FT-IR microspectrometer. A single crystal of each compound was placed on a glass slide, and the spectrum was collected with a diamond attenuated total reflectance (ATR) objective from 650 to 4000 cm^{-1} with a beam aperture of 100 μm.

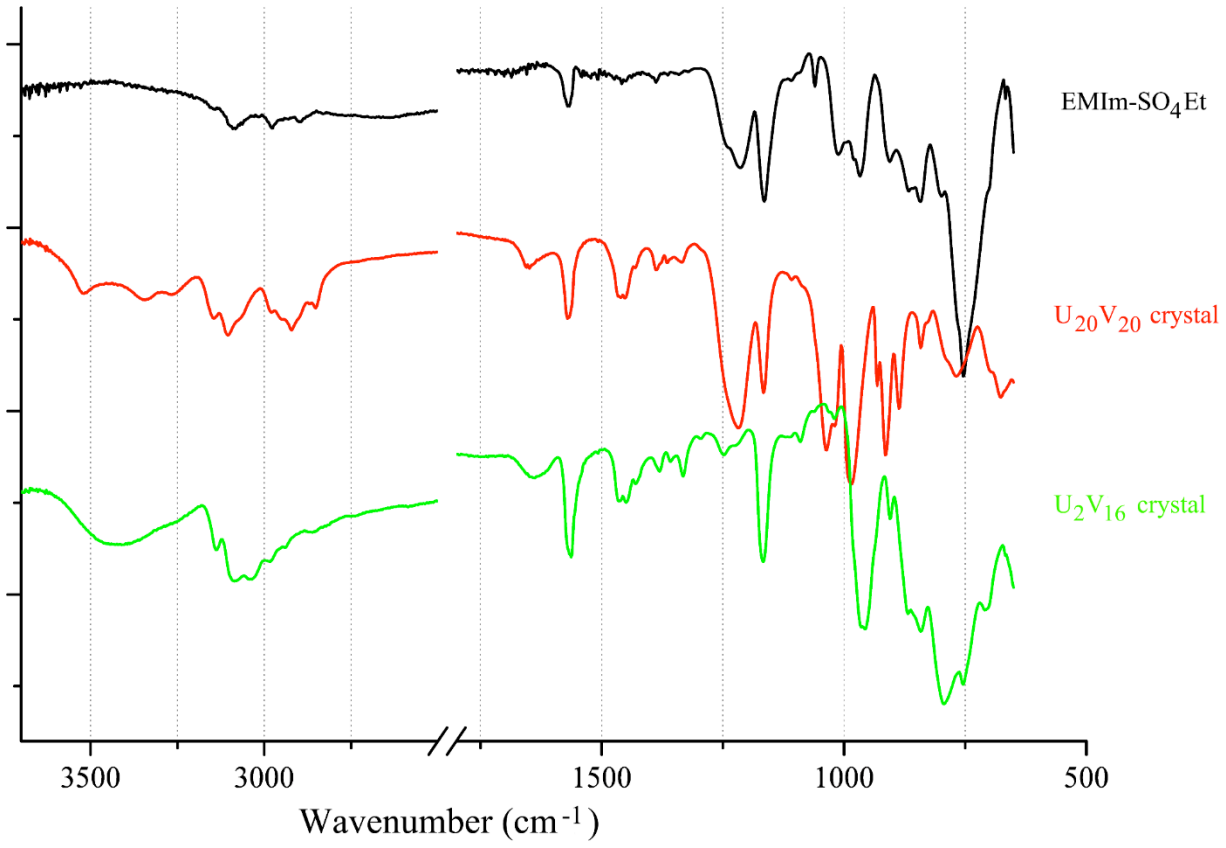

Figure S5. FT-IR spectra of compounds **1a/1b** (*{$U_{20}V_{20}$}* crystals), **2** (*{U_2V_{16}}* crystals) and ionic liquid – EMIm-SO_4Et.

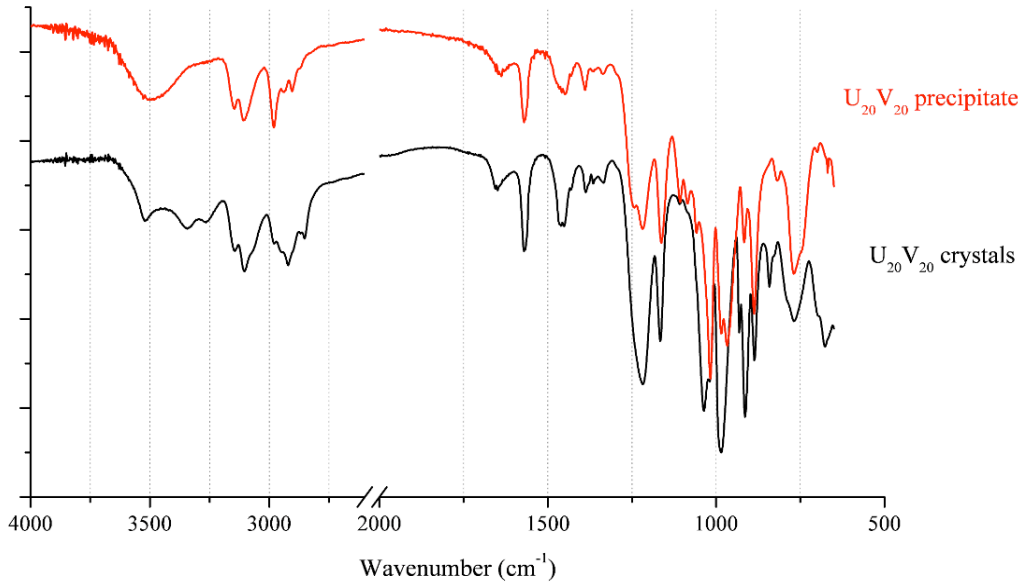

Figure S6. FT-IR spectra of *{U20V20}* crystals (**1a/1b**) and precipitate from *U20V20*-reaction showing presence of uranyl, vanadate and sulfate groups in the precipitate sample.

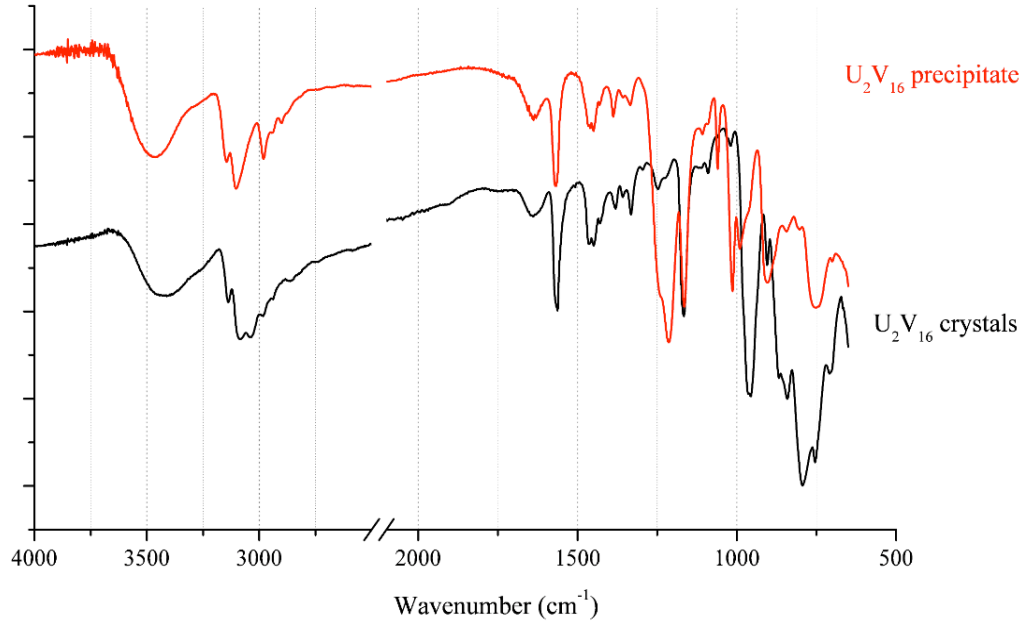

Figure S7. FT-IR spectra of *{U2V16}* crystals (**2**) and precipitate from *U2V16*-reaction showing presence of uranyl, vanadate and sulfate groups in the precipitate sample.

UV-Vis spectroscopy

UV−vis spectra were collected from single crystals using a Craic Technologies microspectro-photometer. The crystals were placed on a glass slide under mineral oil, and the data were collected from 200 to 1500 nm.

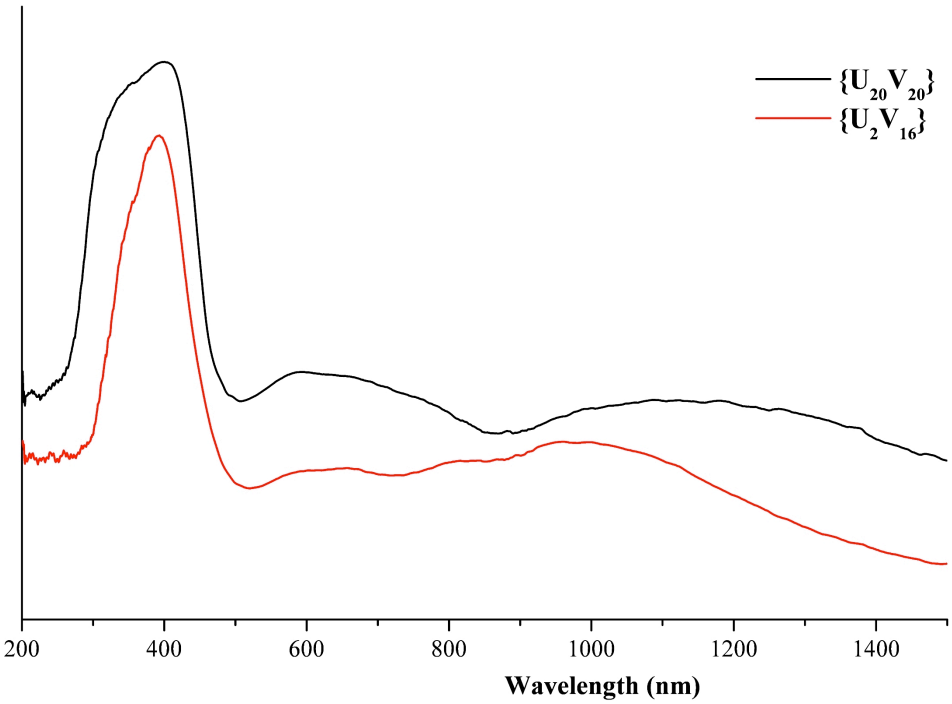

Figure S8. UV-vis spectra of crystals **1a/1b** (*{U20V20}* crystals) and **2** (*{U2V16}* crystals) with intense stretches from uranyl (UO_2^{2+}) and vanadyl (V=O) bonds.

Thermo-gravimetric analysis

TGA measurements were done using a Mettler Toledo thermal analyzer for crystals in Al crucibles under air from room temperature to 500°C with simultaneous mass spectrometric analysis. The small increases of mass observed in some cases near the end of the heat cycles are assumed to be due to capture of oxygen from the atmosphere, likely following the partial reduction and re-oxidation of uranium during the heating cycle.

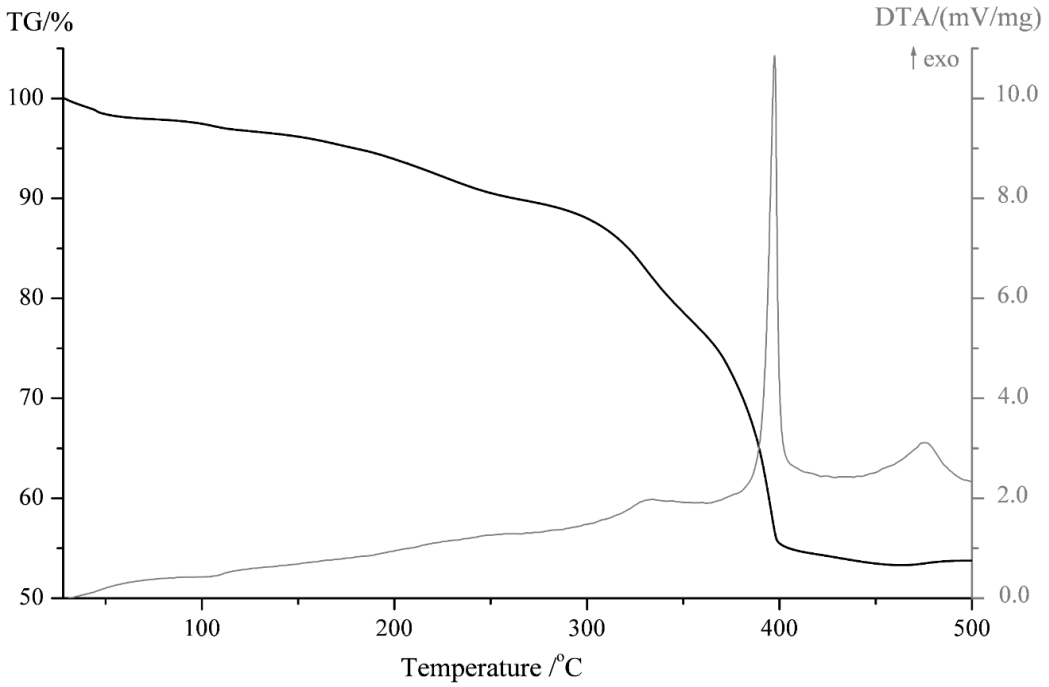

Figure S9. TG and DTA data of compound **1a** (*{U20V20}* crystals) showing a gradual ~10.60% mass loss from room temperature to 265°C corresponding to the release of 70 solvate water molecules (calc. 10.75%), and a more rapid mass loss from 265 to 400°C corresponding to cluster decomposition.

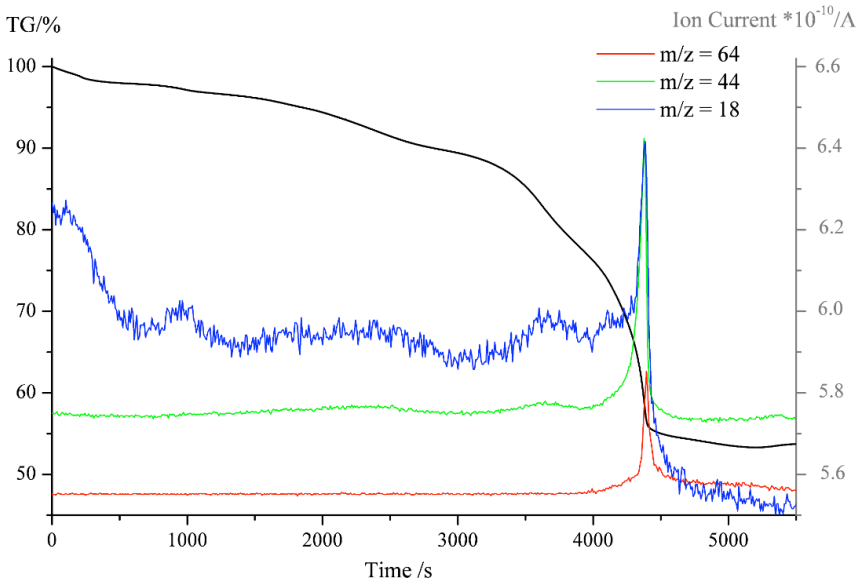

Figure S10. TG data with mass analysis of compound **1a** (*{U20V20}* crystals).

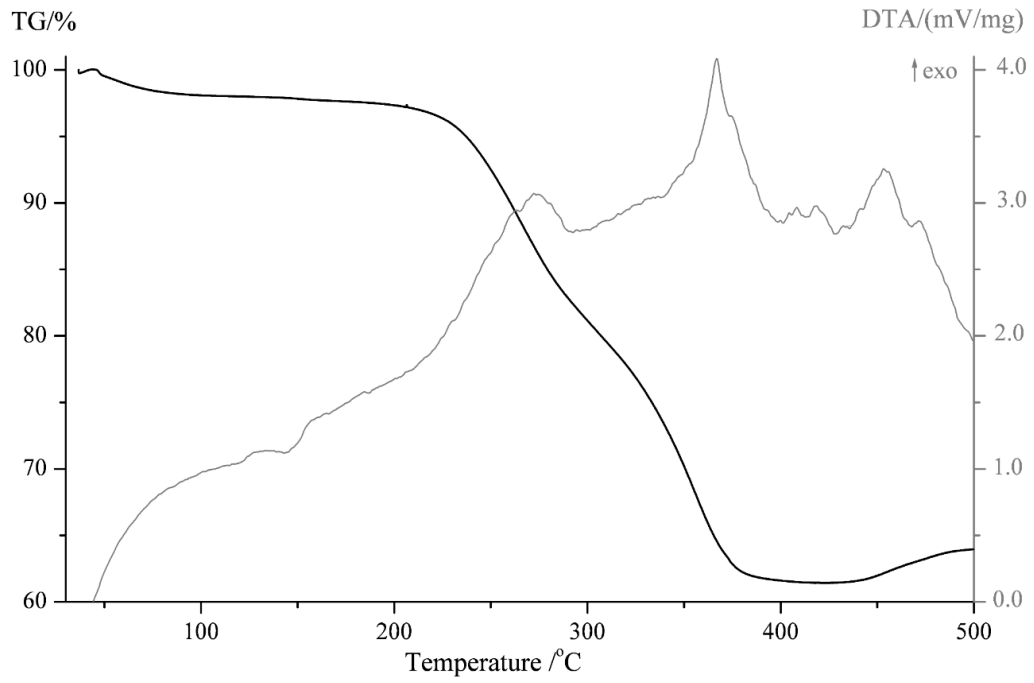

Figure S11. TG and DTA data of compound **2** (U_2V_{16} crystals) showing a gradual mass loss of 2.37% to ~220°C that corresponds to release of 4 water molecules (calc. 2.36%), and decomposition of the compounds from 220 to 400°C.

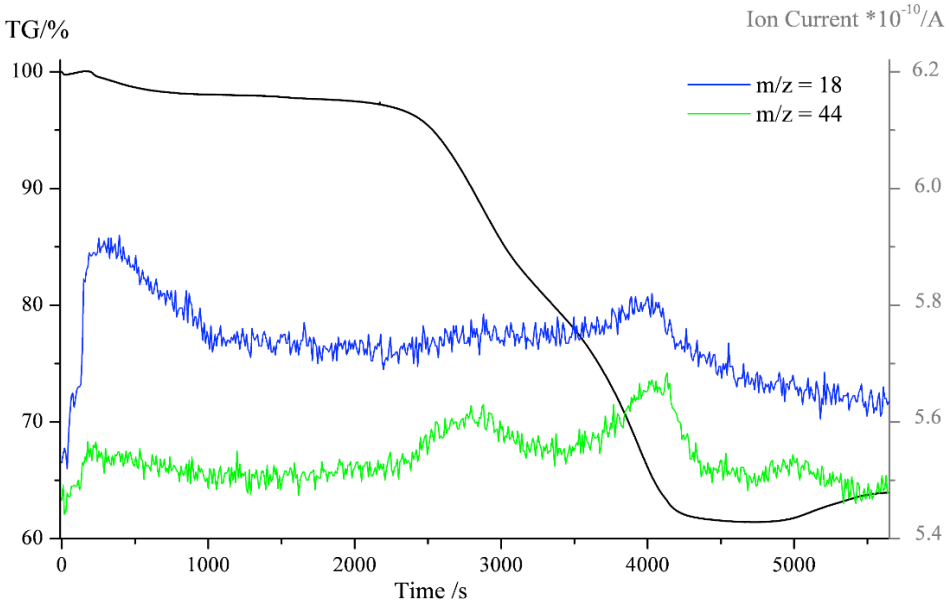

Figure S12. TG data with mass analysis of compound **2** (U_2V_{16} crystals).

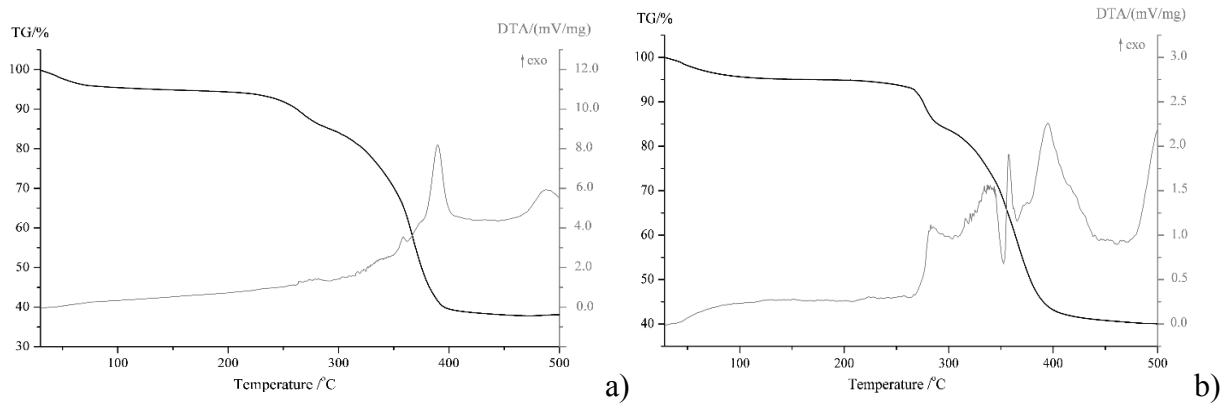

Figure S13. TG and DTA data of precipitates from $U_{20}V_{20}$-reaction (a) and U_2V_{16}-reaction (b).

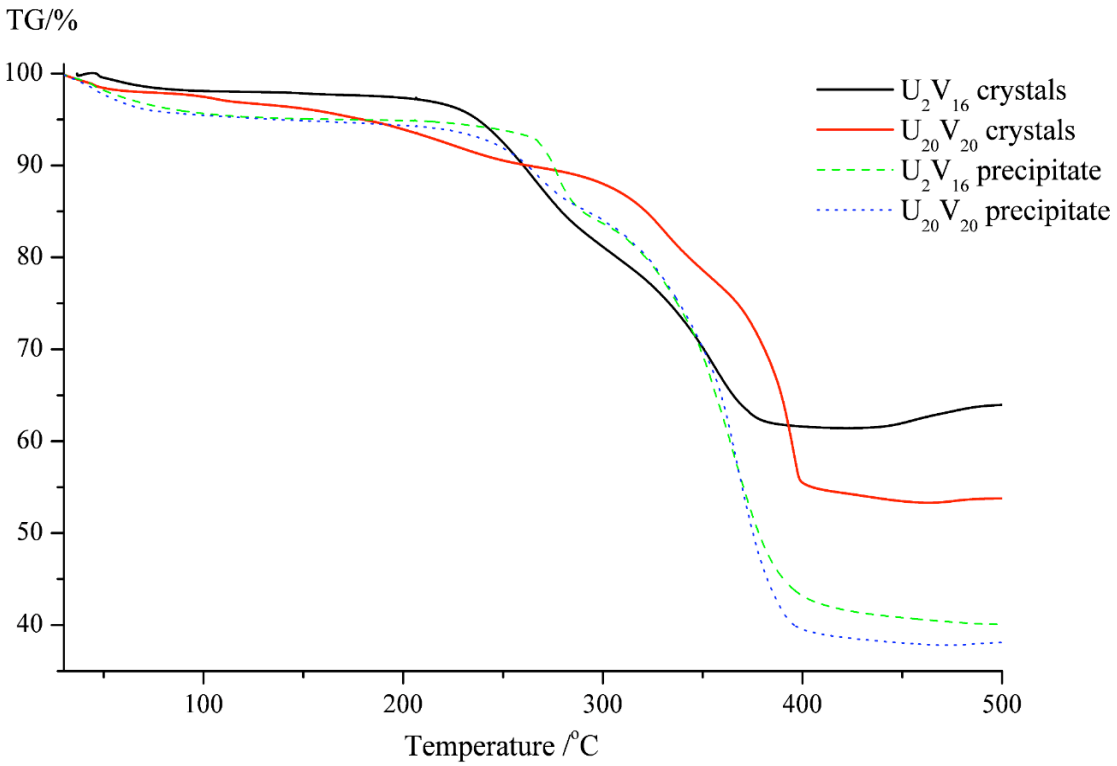

Figure S14. TG data of compounds **1a**, **2** and side products.

Bond-valence sum calculation

Table S2. Bond-valence sum calculations for ***{U20V20}***.

	U1	U2	U3	U4	U5	U6
d_{ij} (U-O, U=O)	1.757	2.333	2.339	2.346	2.352	2.346
	1.785	1.778	2.425	2.323	2.397	1.755
	2.422	1.784	1.774	1.768	1.767	1.775
	2.355	2.347	1.776	1.798	1.764	2.421
	2.419	2.417	2.355	2.334	2.354	2.322
	2.355	2.336	2.413	2.414	2.42	2.322
	2.419	2.316	2.412	2.344	2.403	2.346
V_{ij} (U-O, U=O)	1.75893	0.568527	0.561878	0.554219	0.547737	0.554219
	1.664965	1.687975	0.474688	0.579785	0.501478	1.765842
	0.477488	1.668233	1.701266	1.721399	1.724777	1.697933
	0.544524	0.553133	1.694607	1.623061	1.734953	0.478425
	0.480305	0.482193	0.544524	0.567414	0.545593	0.580923
	0.544524	0.565193	0.485989	0.485037	0.479364	0.580923
	0.480305	0.587798	0.486943	0.556396	0.495613	0.554219
∑	**5.951042**	**6.113051**	**5.949895**	**6.08731**	**6.029515**	**6.212483**

	V1	V2	V3	V4	V5
d_{ij} (V-O, V=O)	1.892	1.876	1.93	1.935	1.904
	1.934	1.874	1.886	1.876	1.886
	1.579	1.924	1.833	1.594	1.865
	1.86	1.615	1.603	1.821	1.61
	1.844	1.828	1.817	1.859	1.82
V_{ij} (V-O, V=O)	0.786203	0.820947	0.709466	0.699943	0.761113
	0.701837	0.825396	0.799056	0.820947	0.799056
	1.831995	0.721064	0.922119	1.75921	0.845719
	0.857226	1.662144	1.716935	0.952516	1.684757
	0.895108	0.934665	0.962869	0.859546	0.955094
∑	**5.072368**	**4.964215**	**5.110444**	**5.092161**	**5.04574**

Bond-valence sums were calculated with the expression $V_{ij} = \exp[(R_{ij} - d_{ij})/B]$[1] (where V_{ij} – bond valence and d_{ij} – bond length between metal center and oxygen atom), using parameters: $R_{ij}(^{[7]}U^{6+}) = 2.045$, $B(^{[7]}U^{6+}) = 0.51$[2]; $R_{ij}(V^{5+}) = 1.803$, $B(V^{5+}) = 0.37$[1].

Table S3. Bond-valence sum calculations for ***{U$_2$V$_{16}$}*** cluster.

	U1	V1	V2	V3	V4
d_{ij} (U-O, U=O)	1.823	1.611	1.602	1.611	1.604
	1.804	1.68	1.713	1.7	1.72
	2.356	1.93	1.889	1.912	1.874
	2.341	1.997	1.987	2.018	1.993
	2.367	1.943	1.932	1.941	1.886
	2.366				
	2.281				
V_{ij} (U-O, U=O)	1.545418	1.68021	1.721581	1.68021	1.712301
	1.604078	1.394356	1.275379	1.320986	1.251477
	0.543457	0.709466	0.792603	0.744833	0.825396
	0.559679	0.591955	0.608172	0.559293	0.598389
	0.531861	0.684971	0.705641	0.688684	0.799056
	0.532905				
	0.629553				
$\sum$	**5.946951**	**5.060958**	**5.103377**	**4.994007**	**5.186619**

	V5	V6	V7	V8
d_{ij} (U-O, U=O)	1.626	1.7	1.625	1.59
	1.936	1.599	1.692	1.687
	1.923	1.881	1.972	1.96
	2.01	2.026	1.925	1.919
	1.703	1.926	1.929	1.975
V_{ij} (U-O, U=O)	1.613456	1.320986	1.617822	1.778332
	0.698054	1.735597	1.349859	1.368224
	0.723016	0.809927	0.633334	0.654212
	0.571518	0.54733	0.719118	0.730875
	1.310319	0.717177	0.711386	0.62822
$\sum$	**4.916362**	**5.131018**	**5.031519**	**5.159862**

Bond-valence sums were calculated with the expression $V_{ij} = \exp[(R_{ij} - d_{ij})/B]$[1] (where V_{ij} – bond valence and d_{ij} – bond length between metal center and oxygen atom), using parameters: $R_{ij}(^{[7]}U^{6+}) = 2.045$, $B(^{[7]}U^{6+}) = 0.51$[2]; $R_{ij}(V^{5+}) = 1.803$, $B(V^{5+}) = 0.37$[1].

X-ray Crystallography

Single crystal X-ray diffraction data was measured at 140 K using a Bruker APEX II CCD detector and a Quazar high intensity micro-focus X-ray source providing Mo-Kα radiation (λ = 0.71073 Å). The Bruker APEX II software[3] was used for data integration, including corrections of Lorentz, polarization, and background effects. SADABS[4] was used for semiempirical absorption corrections. The structures were solved by direct methods and refined using SHELXTL.

Refinement of compound $(EMIm)_{15}Na_5[(UO_2)_{20}(V_2O_7)_{10}(SO_4)_{10}]\cdot 80H_2O$ (1a).

Refinement of the uranyl-vanadate $\{U_{20}V_{20}\}$ cluster structure proceeded normally. Sodium cations inside the cluster possess 0.25 (Na1) and 0.5 (Na2, Na3) occupancy. Only one organic EMIm cation was resolved. CH-hydrogen atoms were added geometrically with $U_{iso} = 1.2U_{eq}$, while H-atoms were not added to water molecules. The other imidazolium counter ions and solvate water molecules are disordered. To model this electron density, the SQUEEZE routine implemented in PLATON [5] was used. This treatment indicates that 20031 $Å^3$ void volume in the structure contains 5412 electrons per unit cell that can be assigned to 10 EMIm cations and 70 solvent water molecules per $\{U_{20}V_{20}\}$ cluster.

Refinement of compound $(EMIm)_{15}Na_5[(UO_2)_{20}(V_2O_7)_{10}(SO_4)_{10}]\cdot nH_2O$ (1b).

Refinement of the uranyl-vanadate $\{U_{20}V_{20}\}$ cluster proceeded normally. The occupancyies of all five independent sodium cations were set to 0.5. It was possible to locate three organic EMIm cations, one of which has 0.5 occupancy. Two EMIm molecules were not stable in refinement, so their geometry, C-N and C-C bond distances were fixed and refined isotropically. H-atoms were not added. The other organic cations were badly disordered, so the SQUEEZE routine implemented in PLATON [5] was used. 1491 electron counts / unit cell were assigned to EMIm cations needed for charge balance.

Refinement of compound *(EMIm)$_8$[(UO$_2$)$_2$(V$_{16}$O$_{46}$)]·4H$_2$O* (2).

Refinement of the uranyl-vanadate *{U$_2$V$_{16}$}* cluster proceeded normally except that there is disorder of the V8 atom. The V8 atom is disordered over two sites with a 0.8 / 0.2 distribution. The V8 atom (0.8 occupancy) was refined anisotropically, but the V8a atom (0.2 occupancy) was refined as isotropic. The disorder was treated without any restraints of the geometry or thermal parameters. All organic EMIm cations were refined anisotropically, and CH-hydrogen atoms were added geometrically with $U_{iso} = 1.2U_{eq}$.

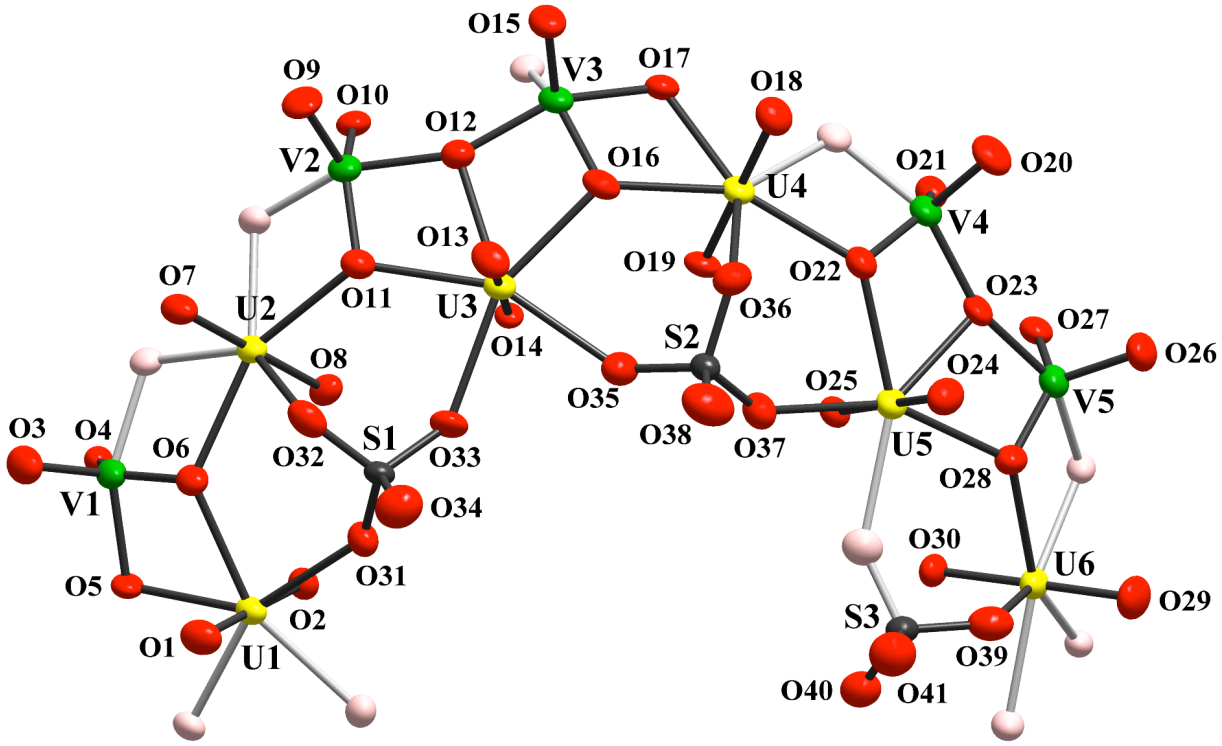

Figure S15. Atom labeling scheme for the *{U$_{20}$V$_{20}$}* cluster in the crystal structure of compound *(EMIm)$_{15}$Na$_5$[(UO$_2$)$_{20}$(V$_2$O$_7$)$_{10}$(SO$_4$)$_{10}$]·80H$_2$O* (**1a**).

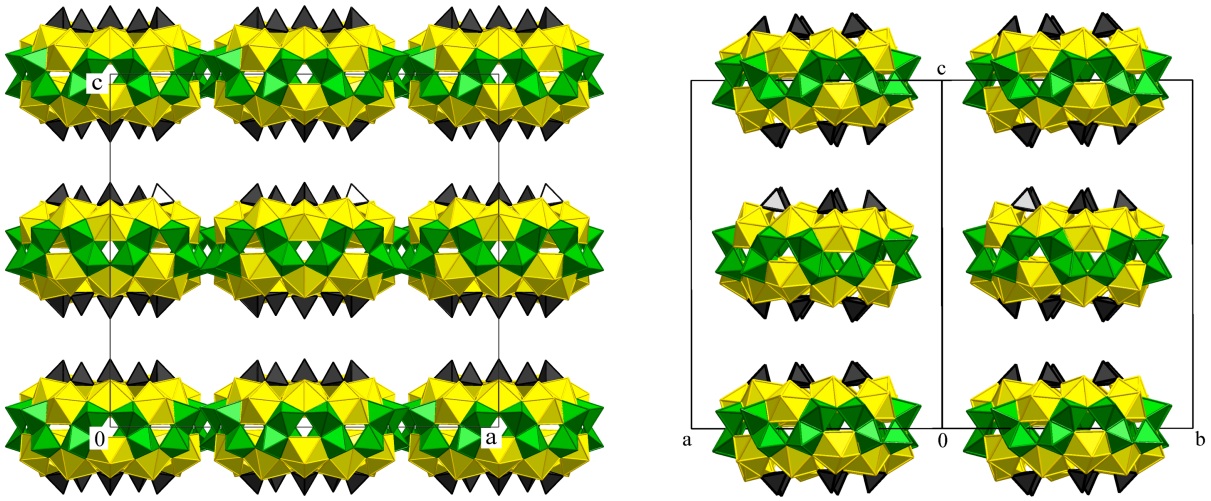

Figure S16. Crystal packing of *{U20V20}* clusters one over another in the crystal structure of **1a**.

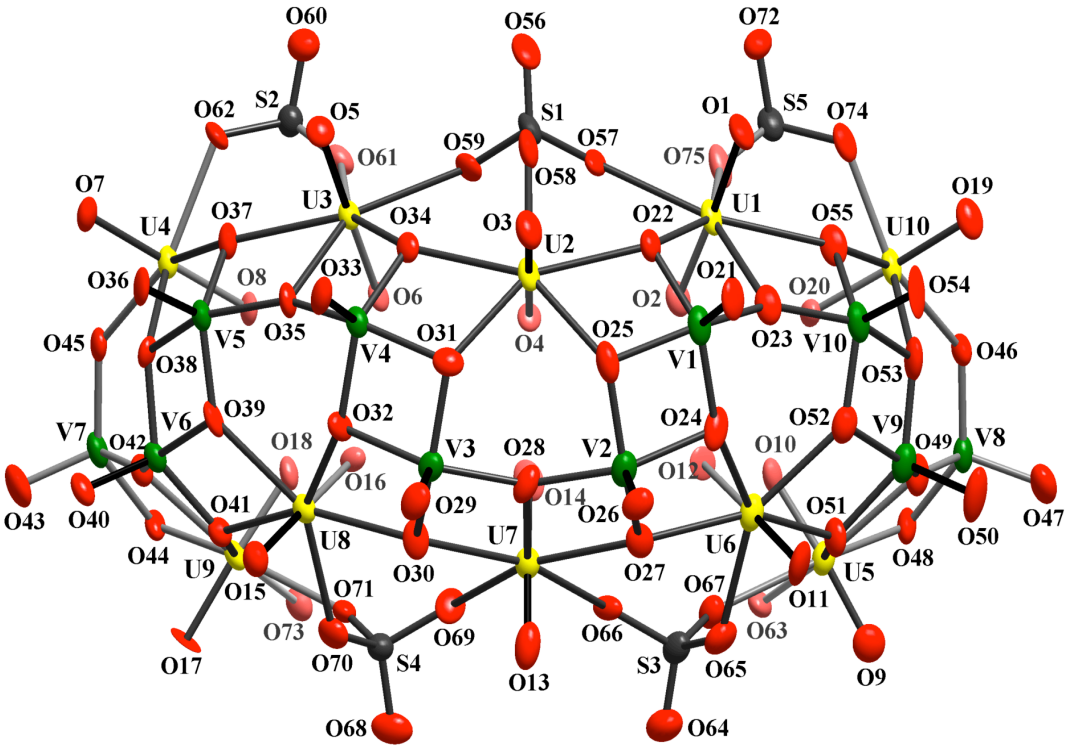

Figure S17. Atom labeling scheme for the *{U20V20}* cluster in the crystal structure of compound *(EMIm)15Na5[(UO2)20(V2O7)10(SO4)10]·nH2O* (**1b**).

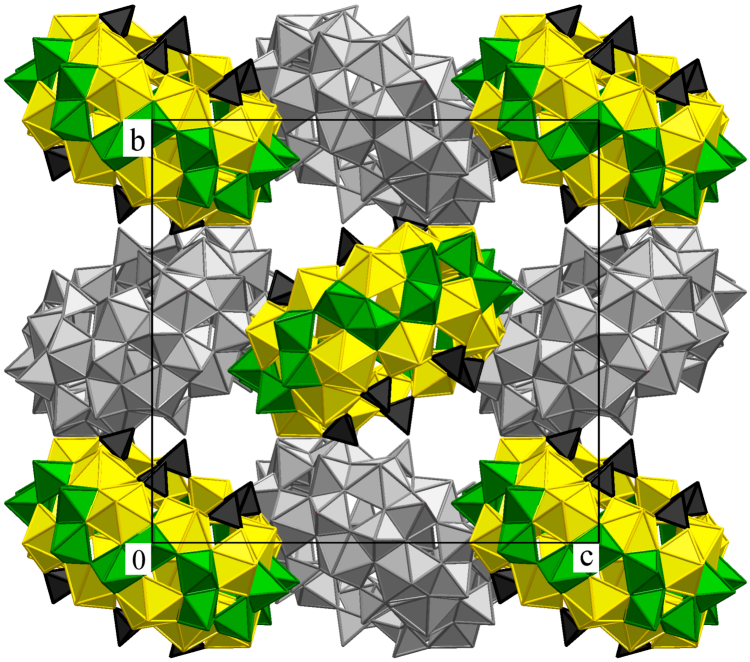

Figure S18. Crystal packing of *{U20V20}* clusters in the crystal structure of **1b**.

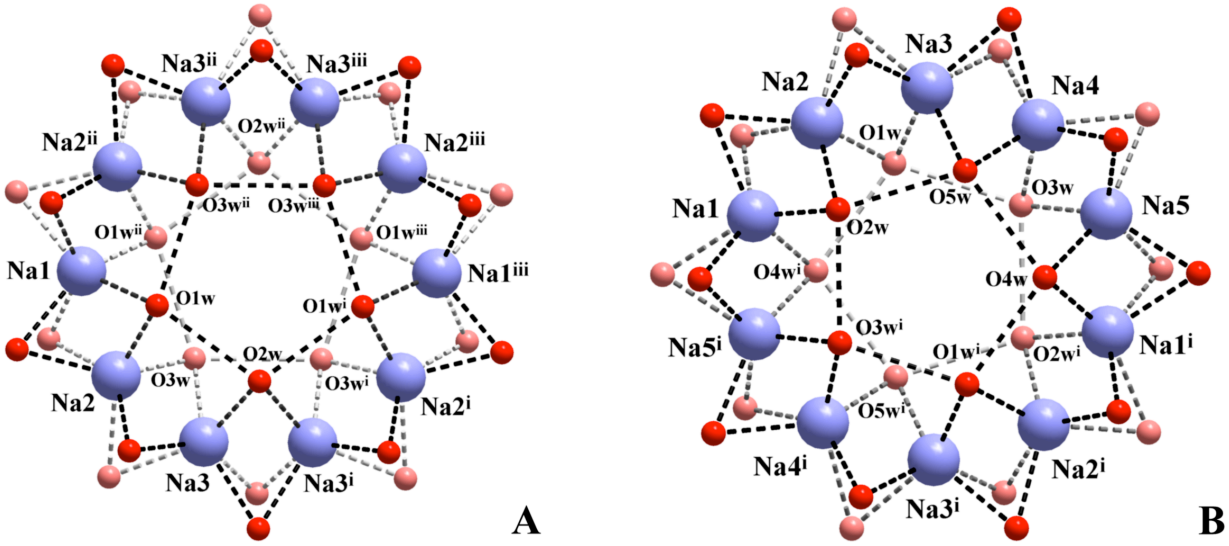

Figure S19. The sodium-aqua "cluster" in **1a** (A) (Symmetry codes: (i) −*x*, *y*, *z*; (ii) *x*, −*y*+1, −*z*+1; (iii) −*x*, −*y*+1, −*z*+1) and **1b** (B) (Symmetry code: (i) −*x*+1, −*y*+1, −*z*+1).

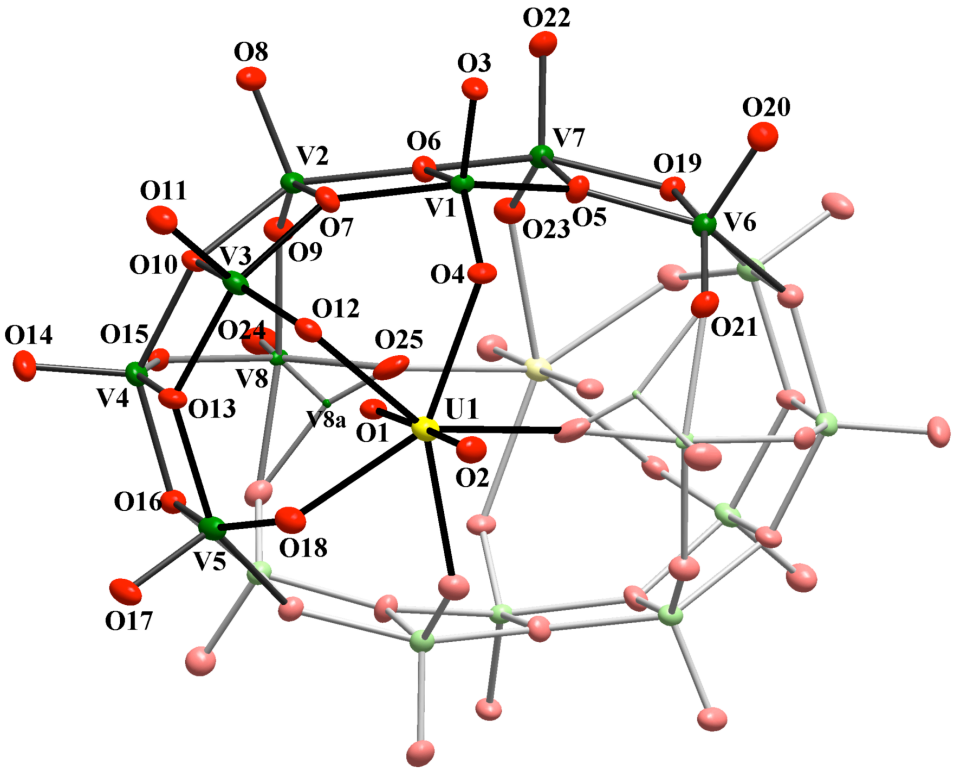

Figure S20. Atom labeling scheme for the *{U_2V_{16}}* cluster in the crystal structure of compound *$(EMIm)_8[(UO_2)_2(V_{16}O_{46})]\cdot 4H_2O$* (**2**).

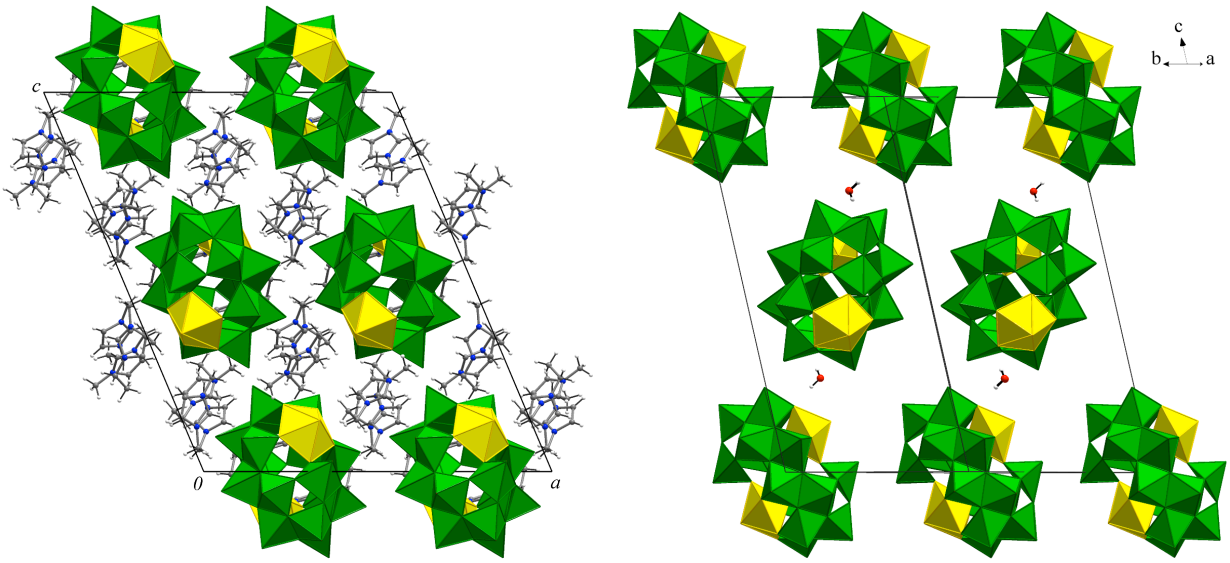

Figure S21. Crystal packing of *{U_2V_{16}}* clusters in the crystal structure **2**.

Table S4. Crystallographic data for *(EMIm)$_{15}$Na$_5$[(UO$_2$)$_{20}$(V$_2$O$_7$)$_{10}$(SO$_4$)$_{10}$]·80H$_2$O* (**1a**), *(EMIm)$_{15}$Na$_5$[(UO$_2$)$_{20}$(V$_2$O$_7$)$_{10}$(SO$_4$)$_{10}$]·nH$_2$O* (**1b**) and *(EMIm)$_8$[(UO$_2$)$_2$(V$_{16}$O$_{46}$)]·4H$_2$O* (**2**).

	1a	**1b**	**2**
Formula	$C_{90}H_{325}N_{30}Na_5O_{230}S_{10}U_{20}V_{20}$	$C_{90}H_{325}N_{30}Na_5O_{230}S_{10}U_{20}V_{20}$	$C_{48}H_{90}N_{16}O_{51}U_2V_{26}$
Molecular mass	11 723.75	10 498.66	2 998.46
Crystal system	Orthorhombic	Orthorhombic	Monoclinic
Space group, *Z*	*C mcm*, 4	*P ccn*, 4	*C 2/c*, 4
a (Å)	35.628(4)	32.023(3)	23.656(4)
b (Å)	29.684(2)	27.232(3)	14.981(2)
c (Å)	32.344(2)	28.774(3)	27.970(4)
α	90	90	90
β	90	90	112.886(2)
γ	90	90	90
V (Å^3)	34207(5)	25092(4)	9132(2)
μ (mm^{-1})	10.117	13.756	5.185
D_c (g/cm^3)	2.276	2.779	2.181
θ_{max} (°)	26.46	26.50	26.69
Total, unique reflns	188670, 13014	169213, 14607	39230, 7571
Parameters refined	585	1135	612
R_{int}	0.1254	0.1110	0.0616
R_1 [I > 2σ(I)]	0.0368	0.0756	0.0636
wR_2 [all data]	0.0830	0.1872	0.1580
Goof on F^2	0.934	1.101	1.101
Max, min peak (e Å^{-3})	1.077, -1.916	3.259, -1.417	2.791, -1.637

Table S5. Selected bond distances (Å) for $(EMIm)_{15}Na_5[(UO_2)_{20}(V_2O_7)_{10}(SO_4)_{10}]\cdot 80H_2O$ (**1a**).

U1—O1	1.753 (7)	U6—O28	2.353 (5)
U1—O2	1.787 (6)	U6—O28i	2.353 (5)
U1—O6i	2.347 (4)	U6—O39	2.426 (8)
U1—O6	2.347 (4)	V1—O3	1.591 (5)
U1—O5	2.420 (7)	V1—O6	1.845 (5)
U1—O31	2.437 (5)	V1—O5	1.859 (2)
U1—O31i	2.437 (5)	V1—O4	1.897 (5)
U2—O7	1.779 (5)	V1—O27	1.929 (5)
U2—O8i	1.787 (4)	V2—O9	1.596 (5)
U2—O27	2.323 (5)	V2—O11	1.823 (5)
U2—O21	2.337 (5)	V2—O12	1.863 (5)
U2—O11	2.343 (5)	V2—O10	1.876 (5)
U2—O6	2.344 (5)	V2—O21	1.909 (5)
U2—O32	2.431 (5)	V3—O15	1.596 (5)
U3—O14i	1.769 (4)	V3—O16	1.808 (5)
U3—O13	1.769 (5)	V3—O12	1.848 (5)
U3—O11	2.344 (5)	V3—O17	1.902 (5)
U3—O16	2.351 (4)	V3—O17ii	1.913 (5)
U3—O35ii	2.410 (5)	V4—O20	1.590 (5)
U3—O12	2.425 (5)	V4—O22	1.812 (5)
U3—O33	2.427 (4)	V4—O23	1.849 (5)
U4—O18	1.771 (5)	V4—O21	1.881 (5)
U4—O19i	1.793 (4)	V4—O10	1.928 (5)
U4—O17	2.319 (5)	V5—O26	1.603 (5)
U4—O22	2.335 (5)	V5—O28	1.818 (5)
U4—O10	2.347 (5)	V5—O23	1.865 (5)
U4—O16ii	2.357 (5)	V5—O27	1.887 (5)
U4—O36	2.413 (5)	V5—O4	1.901 (5)
U5—O24	1.765 (5)	S1—O34	1.423 (6)
U5—O25i	1.773 (4)	S1—O32	1.482 (5)
U5—O22	2.354 (5)	S1—O31	1.496 (5)
U5—O28	2.352 (5)	S1—O33	1.506 (5)
U5—O40	2.411 (5)	S2—O38	1.392 (6)
U5—O23	2.423 (5)	S2—O37	1.501 (5)
U5—O37	2.425 (5)	S2—O36	1.505 (5)
U6—O30	1.779 (6)	S2—O35	1.516 (5)
U6—O29	1.778 (7)	S3—O41	1.417 (9)
U6—O4	2.321 (5)	S3—O39	1.489 (8)
U6—O4i	2.321 (5)	S3—O40	1.506 (5)

Symmetry codes: (i) $-x, y, z$; (ii) $x, -y+1, -z+1$.

Table S6. Selected angles (°) for *(EMIm)$_{15}$Na$_5$[(UO$_2$)$_{20}$(V$_2$O$_7$)$_{10}$(SO$_4$)$_{10}$]·80H$_2$O* (**1a**).

O1—U1—O2	178.6 (3)	O14i—U3—O11	92.40 (18)
O1—U1—O6i	87.61 (17)	O13—U3—O11	88.2 (2)
O2—U1—O6i	93.00 (15)	O14i—U3—O16	93.18 (18)
O1—U1—O6	87.61 (17)	O13—U3—O16	88.31 (19)
O2—U1—O6	93.00 (15)	O11—U3—O16	125.45 (16)
O6i—U1—O6	126.3 (2)	O14i—U3—O35ii	84.96 (19)
O1—U1—O5	96.7 (3)	O13—U3—O35ii	93.6 (2)
O2—U1—O5	84.6 (3)	O11—U3—O35ii	154.20 (16)
O6i—U1—O5	63.78 (12)	O16—U3—O35ii	80.34 (16)
O6—U1—O5	63.78 (12)	O14i—U3—O12	84.29 (18)
O1—U1—O31	93.6 (2)	O13—U3—O12	98.0 (2)
O2—U1—O31	85.3 (2)	O11—U3—O12	63.69 (16)
O6i—U1—O31	153.74 (16)	O16—U3—O12	63.01 (16)
O6—U1—O31	79.96 (16)	O35ii—U3—O12	141.01 (16)
O5—U1—O31	141.67 (13)	O14i—U3—O33	84.54 (18)
O1—U1—O31i	93.6 (2)	O13—U3—O33	93.4 (2)
O2—U1—O31i	85.3 (2)	O11—U3—O33	79.38 (16)
O6i—U1—O31i	79.96 (16)	O16—U3—O33	155.17 (17)
O6—U1—O31i	153.74 (16)	O35ii—U3—O33	74.82 (16)
O5—U1—O31i	141.67 (13)	O12—U3—O33	140.78 (17)
O31—U1—O31i	73.8 (2)	O18—U4—O19i	179.4 (2)
O7—U2—O8i	179.1 (2)	O18—U4—O17	87.6 (2)
O7—U2—O27	88.6 (2)	O19i—U4—O17	91.78 (19)
O8i—U2—O27	92.06 (19)	O18—U4—O22	94.6 (2)
O7—U2—O21	88.82 (19)	O19i—U4—O22	86.01 (19)
O8i—U2—O21	91.87 (18)	O17—U4—O22	145.75 (17)
O27—U2—O21	78.46 (16)	O18—U4—O10	87.9 (2)
O7—U2—O11	93.73 (19)	O19i—U4—O10	92.11 (18)
O8i—U2—O11	86.03 (19)	O17—U4—O10	79.46 (16)
O27—U2—O11	144.57 (17)	O22—U4—O10	66.50 (17)
O21—U2—O11	66.27 (16)	O18—U4—O16ii	94.0 (2)
O7—U2—O6	93.61 (19)	O19i—U4—O16ii	85.59 (18)
O8i—U2—O6	86.15 (18)	O17—U4—O16ii	65.70 (16)
O27—U2—O6	66.85 (17)	O22—U4—O16ii	147.68 (16)
O21—U2—O6	145.13 (17)	O10—U4—O16ii	144.96 (17)
O11—U2—O6	147.86 (17)	O18—U4—O36	83.9 (2)
O7—U2—O32	83.7 (2)	O19i—U4—O36	96.41 (19)
O8i—U2—O32	95.45 (19)	O17—U4—O36	139.03 (17)
O27—U2—O32	140.20 (16)	O22—U4—O36	75.04 (17)
O21—U2—O32	139.99 (16)	O10—U4—O36	139.86 (17)
O11—U2—O32	75.06 (16)	O16ii—U4—O36	74.98 (17)
O6—U2—O32	74.73 (17)	O24—U5—O25i	178.3 (2)
O27—U2—V2	112.65 (12)	O24—U5—O22	87.9 (2)
O14i—U3—O13	177.7 (2)	O25i—U5—O22	92.37 (19)

(continuation)

O24—U5—O28	87.8 (2)
O25i—U5—O28	93.4 (2)
O22—U5—O28	125.83 (16)
O24—U5—O40	94.1 (2)
O25i—U5—O40	84.94 (19)
O22—U5—O40	154.27 (17)
O28—U5—O40	79.90 (17)
O24—U5—O23	96.6 (2)
O25i—U5—O23	85.01 (19)
O22—U5—O23	63.52 (16)
O28—U5—O23	63.44 (16)
O40—U5—O23	141.22 (17)
O24—U5—O37	93.0 (2)
O25i—U5—O37	85.41 (19)
O22—U5—O37	79.61 (16)
O28—U5—O37	154.56 (16)
O40—U5—O37	74.67 (17)
O23—U5—O37	141.36 (16)
O30—U6—O29	179.0 (4)
O30—U6—O4	91.6 (2)
O29—U6—O4	89.2 (2)
O30—U6—O4i	91.6 (2)
O29—U6—O4i	89.2 (2)
O4—U6—O4i	79.9 (2)
O30—U6—O28	85.92 (14)
O29—U6—O28	93.80 (14)
O4—U6—O28	65.97 (17)
O4i—U6—O28	145.66 (17)
O30—U6—O28i	85.92 (14)
O29—U6—O28i	93.80 (14)
O4—U6—O28i	145.66 (17)
O4i—U6—O28i	65.97 (17)
O28—U6—O28i	147.5 (3)
O30—U6—O39	95.6 (3)
O29—U6—O39	83.3 (3)
O4—U6—O39	139.43 (12)
O4i—U6—O39	139.43 (12)
O28—U6—O39	74.80 (13)
O28i—U6—O39	74.80 (13)
O3—V1—O6	109.3 (3)
O3—V1—O5	106.0 (3)
O6—V1—O5	85.7 (3)
O3—V1—O4	109.2 (3)
O6—V1—O4	140.7 (2)
O5—V1—O4	90.8 (3)
O3—V1—O27	103.2 (2)
O6—V1—O27	85.8 (2)
O5—V1—O27	150.7 (3)
O4—V1—O27	78.4 (2)
O9—V2—O11	109.7 (3)
O9—V2—O12	106.3 (3)
O11—V2—O12	86.1 (2)
O9—V2—O10	108.0 (3)
O11—V2—O10	141.9 (2)
O12—V2—O10	89.1 (2)
O9—V2—O21	103.9 (2)
O11—V2—O21	86.5 (2)
O12—V2—O21	149.6 (2)
O10—V2—O21	78.8 (2)
O15—V3—O16	109.6 (3)
O15—V3—O12	105.1 (2)
O16—V3—O12	86.1 (2)
O15—V3—O17	108.7 (3)
O16—V3—O17	141.1 (2)
O12—V3—O17	90.3 (2)
O15—V3—O17ii	104.0 (2)
O16—V3—O17ii	85.9 (2)
O12—V3—O17ii	150.8 (2)
O17—V3—O17ii	78.6 (2)
O20—V4—O22	109.8 (3)
O20—V4—O23	104.7 (3)
O22—V4—O23	86.8 (2)
O20—V4—O21	110.1 (3)
O22—V4—O21	139.6 (2)
O23—V4—O21	89.4 (2)
O20—V4—O10	103.3 (2)
O22—V4—O10	86.6 (2)
O23—V4—O10	151.8 (2)
O21—V4—O10	78.2 (2)
O26—V5—O28	109.6 (3)
O26—V5—O23	104.9 (3)
O28—V5—O23	86.0 (2)
O26—V5—O27	109.0 (3)
O28—V5—O27	141.0 (2)
O23—V5—O27	89.7 (2)
O26—V5—O4	103.7 (2)
O28—V5—O4	86.3 (2)
O23—V5—O4	151.4 (2)
O27—V5—O4	79.3 (2)
V1—O4—V5	101.5 (2)
V1—O4—U6	138.9 (2)
V5—O4—U6	103.1 (2)

(continuation)

V1—O5—V1i	153.7 (5)	V3—O17—V3ii	101.4 (2)
V1—O5—U1	102.8 (2)	V3—O17—U4	137.4 (2)
V1i—O5—U1	102.8 (2)	V3ii—O17—U4	103.2 (2)
V1—O6—U2	104.6 (2)	V4—O21—V2	101.7 (2)
V1—O6—U1	106.1 (2)	V4—O21—U2	140.2 (2)
U2—O6—U1	131.2 (2)	V2—O21—U2	102.3 (2)
V2—O10—V4	101.2 (2)	V4—O22—U4	105.5 (2)
V2—O10—U4	138.3 (2)	V4—O22—U5	106.2 (2)
V4—O10—U4	101.3 (2)	U4—O22—U5	132.4 (2)
V2—O11—U2	104.9 (2)	V4—O23—V5	154.8 (3)
V2—O11—U3	106.8 (2)	V4—O23—U5	102.3 (2)
U2—O11—U3	132.0 (2)	V5—O23—U5	102.4 (2)
V3—O12—V2	154.7 (3)	V5—O27—V1	100.8 (2)
V3—O12—U3	102.8 (2)	V5—O27—U2	139.6 (2)
V2—O12—U3	102.3 (2)	V1—O27—U2	102.7 (2)
V3—O16—U3	107.0 (2)	V5—O28—U6	104.6 (2)
V3—O16—U4ii	105.2 (2)	V5—O28—U5	106.7 (2)
U3—O16—U4ii	131.37 (19)	U6—O28—U5	131.5 (2)

Symmetry codes: (i) $-x, y, z$; (ii) $x, -y+1, -z+1$.

Table S7. Selected bond distances (Å) for *(EMIm)$_{15}$Na$_5$[(UO$_2$)$_{20}$(V$_2$O$_7$)$_{10}$(SO$_4$)$_{10}$]·nH$_2$O* (**1b**).

U1—O1	1.816 (12)	U4—O7	1.817 (12)
U1—O2	1.779 (13)	U4—O45	2.292 (12)
U1—O22	2.313 (13)	U4—O37	2.302 (12)
U1—O23	2.401 (16)	U4—O38	2.308 (13)
U1—O55	2.362 (13)	U4—O48i	2.323 (15)
U1—O75	2.388 (15)	U4—O62	2.433 (12)
U1—O57	2.421 (13)	U5—O9	1.757 (16)
U2—O4	1.767 (11)	U5—O10	1.784 (14)
U2—O3	1.781 (13)	U5—O51	2.325 (13)
U2—O25	2.273 (16)	U5—O48	2.350 (14)
U2—O31	2.307 (13)	U5—O49	2.382 (14)
U2—O34	2.356 (12)	U5—O63	2.399 (13)
U2—O22	2.368 (12)	U5—O67	2.430 (13)
U2—O58	2.362 (16)	U6—O11	1.813 (14)
U3—O5	1.768 (12)	U6—O12	1.810 (12)
U3—O6	1.771 (11)	U6—O24	2.313 (13)
U3—O34	2.320 (12)	U6—O27	2.339 (13)
U3—O37	2.375 (11)	U6—O51	2.322 (12)
U3—O35	2.367 (13)	U6—O52	2.331 (15)
U3—O59	2.438 (11)	U6—O65	2.451 (15)
U3—O61	2.436 (14)	U7—O13	1.69 (2)
U4—O8	1.797 (11)	U7—O14	1.727 (17)

(continuation)

U7—O27	2.334 (12)	V5—O36	1.611 (11)
U7—O30	2.344 (13)	V5—O37	1.812 (14)
U7—O28	2.381 (13)	V5—O35	1.817 (12)
U7—O69	2.395 (12)	V5—O39	1.849 (15)
U7—O66	2.415 (11)	V5—O38	1.910 (11)
U8—O15	1.791 (15)	V6—O40	1.631 (12)
U8—O16	1.794 (12)	V6—O41	1.805 (13)
U8—O32	2.326 (11)	V6—O42	1.867 (12)
U8—O39	2.336 (14)	V6—O38	1.907 (13)
U8—O30	2.352 (13)	V6—O39	1.956 (11)
U8—O41	2.350 (12)	V7—O43	1.623 (14)
U8—O70	2.427 (14)	V7—O42	1.837 (13)
U9—O18	1.781 (13)	V7—O44	1.843 (13)
U9—O17	1.795 (11)	V7—O46i	1.886 (14)
U9—O44	2.328 (14)	V7—O45	1.921 (14)
U9—O41	2.350 (11)	V8—O47	1.596 (16)
U9—O42	2.392 (12)	V8—O48	1.786 (13)
U9—O71	2.397 (13)	V8—O49	1.830 (16)
U9—O73	2.431 (12)	V8—O46	1.901 (13)
U10—O19	1.773 (12)	V8—O45i	1.909 (14)
U10—O20	1.767 (12)	V9—O50	1.629 (15)
U10—O46	2.318 (12)	V9—O51	1.864 (15)
U10—O55	2.327 (12)	V9—O49	1.880 (15)
U10—O44i	2.337 (14)	V9—O53	1.885 (18)
U10—O53	2.346 (16)	V9—O52	1.926 (13)
U10—O74	2.385 (15)	V10—O54	1.623 (12)
V1—O21	1.615 (12)	V10—O55	1.801 (17)
V1—O23	1.836 (14)	V10—O52	1.856 (16)
V1—O22	1.867 (15)	V10—O23	1.889 (13)
V1—O25	1.887 (14)	V10—O53	1.906 (13)
V1—O24	1.897 (16)	S1—O56	1.409 (19)
V2—O26	1.618 (14)	S1—O59	1.480 (13)
V2—O27	1.829 (14)	S1—O57	1.493 (14)
V2—O28	1.863 (14)	S1—O58	1.513 (15)
V2—O24	1.927 (15)	S2—O60	1.371 (16)
V2—O25	1.951 (18)	S2—O62	1.463 (12)
V3—O29	1.587 (15)	S2—O61	1.461 (15)
V3—O30	1.821 (14)	S2—O63i	1.515 (15)
V3—O28	1.846 (13)	S3—O64	1.413 (18)
V3—O31	1.897 (14)	S3—O67	1.460 (14)
V3—O32	1.914 (13)	S3—O65	1.461 (15)
V4—O33	1.627 (13)	S3—O66	1.482 (13)
V4—O34	1.805 (13)	S4—O68	1.493 (16)
V4—O35	1.898 (13)	S4—O70	1.489 (13)
V4—O32	1.895 (14)	S4—O71	1.500 (15)
V4—O31	1.898 (14)	S4—O69	1.509 (15)

(continuation)

S5—O73i	1.474 (13)	S5—O75	1.490 (15)
S5—O72	1.456 (15)	S5—O74	1.503 (14)

Symmetry code: (i) −*x*+1, −*y*+1, −*z*+1.

Table S8. Selected angles (°) for *(EMIm)$_{15}$Na$_5$[(UO$_2$)$_{20}$(V$_2$O$_7$)$_{10}$(SO$_4$)$_{10}$]·nH$_2$O* (**1b**).

O2—U1—O1	176.6(7)	O25—U2—O58	139.8(5)
O2—U1—O22	93.1(5)	O31—U2—O58	138.4(4)
O1—U1—O22	87.8(5)	O34—U2—O58	74.9(4)
O2—U1—O55	94.4(5)	O22—U2—O58	74.8(4)
O1—U1—O55	87.7(5)	O5—U3—O6	177.5(6)
O22—U1—O55	125.4(5)	O5—U3—O34	88.5(5)
O2—U1—O23	85.1(5)	O6—U3—O34	93.7(5)
O1—U1—O23	98.2(6)	O5—U3—O37	88.1(5)
O22—U1—O23	63.7(4)	O6—U3—O37	91.7(5)
O55—U1—O23	63.2(5)	O34—U3—O37	126.0(4)
O2—U1—O75	84.4(5)	O5—U3—O35	96.7(6)
O1—U1—O75	93.4(6)	O6—U3—O35	85.4(5)
O22—U1—O75	153.8(5)	O34—U3—O35	64.2(4)
O55—U1—O75	80.8(5)	O37—U3—O35	62.8(4)
O23—U1—O75	141.5(5)	O5—U3—O59	94.4(5)
O2—U1—O57	85.4(5)	O6—U3—O59	84.7(5)
O1—U1—O57	91.5(6)	O34—U3—O59	80.1(4)
O22—U1—O57	79.7(5)	O37—U3—O59	153.9(4)
O55—U1—O57	154.8(5)	O35—U3—O59	142.1(4)
O23—U1—O57	141.6(5)	O5—U3—O61	92.5(5)
O75—U1—O57	74.1(5)	O6—U3—O61	85.0(5)
O4—U2—O3	178.6(7)	O34—U3—O61	154.9(4)
O4—U2—O25	91.7(5)	O37—U3—O61	79.1(4)
O3—U2—O25	89.1(6)	O35—U3—O61	140.3(4)
O4—U2—O31	91.2(5)	O59—U3—O61	74.8(4)
O3—U2—O31	90.1(5)	O8—U4—O7	179.4(6)
O25—U2—O31	80.5(5)	O8—U4—O45	91.5(5)
O4—U2—O34	85.0(5)	O7—U4—O45	88.9(5)
O3—U2—O34	95.1(5)	O8—U4—O37	84.9(5)
O25—U2—O34	145.3(5)	O7—U4—O37	94.5(5)
O31—U2—O34	65.0(5)	O45—U4—O37	145.5(5)
O4—U2—O22	86.4(5)	O8—U4—O38	90.6(5)
O3—U2—O22	92.8(5)	O7—U4—O38	89.1(5)
O25—U2—O22	66.4(5)	O45—U4—O38	79.9(4)
O31—U2—O22	146.7(5)	O37—U4—O38	65.9(4)
O34—U2—O22	147.3(5)	O8—U4—O48i	86.7(5)
O4—U2—O58	95.8(5)	O7—U4—O48i	93.9(5)
O3—U2—O58	82.8(6)	O45—U4—O48i	65.3(5)

(continuation)

O37—U4—O48i	148.0(5)
O38—U4—O48i	145.0(4)
O8—U4—O62	96.1(5)
O7—U4—O62	83.9(6)
O45—U4—O62	140.2(5)
O37—U4—O62	74.2(5)
O38—U4—O62	138.7(4)
O48i—U4—O62	76.1(5)
O9—U5—O10	176.4(6)
O9—U5—O51	87.8(6)
O10—U5—O51	93.1(6)
O9—U5—O48	89.2(6)
O10—U5—O48	93.0(6)
O51—U5—O48	126.6(4)
O9—U5—O49	99.0(6)
O10—U5—O49	84.5(5)
O51—U5—O49	65.0(5)
O48—U5—O49	62.9(5)
O9—U5—O63	92.7(6)
O10—U5—O63	84.9(5)
O51—U5—O63	152.0(5)
O48—U5—O63	81.4(4)
O49—U5—O63	142.1(5)
O9—U5—O67	91.8(6)
O10—U5—O67	85.0(5)
O51—U5—O67	80.0(5)
O48—U5—O67	153.4(4)
O49—U5—O67	142.7(5)
O63—U5—O67	72.0(5)
O11—U6—O12	178.3(7)
O11—U6—O24	87.6(6)
O12—U6—O24	93.1(5)
O11—U6—O27	93.4(5)
O12—U6—O27	85.4(5)
O24—U6—O27	66.8(5)
O11—U6—O51	94.6(6)
O12—U6—O51	85.7(5)
O24—U6—O51	145.8(5)
O27—U6—O51	146.6(5)
O11—U6—O52	89.6(6)
O12—U6—O52	92.1(5)
O24—U6—O52	78.5(5)
O27—U6—O52	145.0(5)
O51—U6—O52	67.4(5)
O11—U6—O65	83.9(6)
O12—U6—O65	94.6(5)
O24—U6—O65	139.2(5)
O27—U6—O65	73.9(5)
O51—U6—O65	74.8(5)
O52—U6—O65	141.0(5)
O13—U7—O14	177.3(6)
O13—U7—O27	86.8(6)
O14—U7—O27	94.0(6)
O13—U7—O30	87.5(6)
O14—U7—O30	94.2(6)
O27—U7—O30	125.4(4)
O13—U7—O28	97.9(6)
O14—U7—O28	84.8(5)
O27—U7—O28	64.0(5)
O30—U7—O28	63.1(5)
O13—U7—O69	94.0(6)
O14—U7—O69	84.1(6)
O27—U7—O69	154.1(5)
O30—U7—O69	80.5(4)
O28—U7—O69	141.0(5)
O13—U7—O66	92.9(6)
O14—U7—O66	84.7(5)
O27—U7—O66	78.9(4)
O30—U7—O66	155.7(4)
O28—U7—O66	140.6(5)
O69—U7—O66	75.2(5)
O15—U8—O16	178.9(6)
O15—U8—O32	87.8(6)
O16—U8—O32	93.3(5)
O15—U8—O39	90.9(6)
O16—U8—O39	89.6(5)
O32—U8—O39	78.4(4)
O15—U8—O30	92.9(6)
O16—U8—O30	87.3(5)
O32—U8—O30	66.6(5)
O39—U8—O30	144.6(4)
O15—U8—O41	94.2(5)
O16—U8—O41	85.0(5)
O32—U8—O41	145.6(5)
O39—U8—O41	67.2(4)
O30—U8—O41	147.3(4)
O15—U8—O70	83.3(5)
O16—U8—O70	95.7(5)
O32—U8—O70	139.6(5)
O39—U8—O70	140.8(4)
O30—U8—O70	74.6(5)
O41—U8—O70	74.6(5)

(continuation)

O18—U9—O17	177.2(6)	O23—V1—O25	150.1(6)
O18—U9—O44	93.9(5)	O22—V1—O25	85.2(7)
O17—U9—O44	88.3(6)	O21—V1—O24	108.6(7)
O18—U9—O41	93.4(5)	O23—V1—O24	89.7(7)
O17—U9—O41	86.8(5)	O22—V1—O24	142.0(6)
O44—U9—O41	126.4(4)	O25—V1—O24	81.4(7)
O18—U9—O42	85.6(5)	O26—V2—O27	109.8(7)
O17—U9—O42	97.0(6)	O26—V2—O28	106.0(7)
O44—U9—O42	64.0(4)	O27—V2—O28	85.3(6)
O41—U9—O42	63.7(4)	O26—V2—O24	104.1(7)
O18—U9—O71	85.3(5)	O27—V2—O24	85.9(6)
O17—U9—O71	92.0(6)	O28—V2—O24	149.9(6)
O44—U9—O71	152.8(4)	O26—V2—O25	110.1(7)
O41—U9—O71	80.8(5)	O27—V2—O25	139.7(6)
O42—U9—O71	142.7(4)	O28—V2—O25	89.3(6)
O18—U9—O73	84.7(5)	O24—V2—O25	79.1(6)
O17—U9—O73	93.8(5)	O29—V3—O30	108.4(8)
O44—U9—O73	79.5(4)	O29—V3—O28	105.7(7)
O41—U9—O73	154.1(5)	O30—V3—O28	84.8(6)
O42—U9—O73	141.5(5)	O29—V3—O31	110.5(7)
O71—U9—O73	73.3(5)	O30—V3—O31	140.6(6)
O19—U10—O20	177.4(6)	O28—V3—O31	90.6(6)
O19—U10—O46	89.4(5)	O29—V3—O32	103.4(7)
O20—U10—O46	92.9(5)	O30—V3—O32	86.8(6)
O19—U10—O55	93.2(5)	O28—V3—O32	150.9(6)
O20—U10—O55	84.2(5)	O31—V3—O32	78.4(6)
O46—U10—O55	145.1(5)	O33—V4—O34	111.4(7)
O19—U10—O44i	93.9(5)	O33—V4—O35	106.2(6)
O20—U10—O44i	88.2(5)	O34—V4—O35	84.4(6)
O46—U10—O44i	66.7(5)	O33—V4—O32	107.5(7)
O55—U10—O44i	147.5(5)	O34—V4—O32	140.4(6)
O19—U10—O53	88.7(6)	O35—V4—O32	91.5(6)
O20—U10—O53	90.4(6)	O33—V4—O31	104.0(6)
O46—U10—O53	79.7(5)	O34—V4—O31	85.1(6)
O55—U10—O53	65.6(5)	O35—V4—O31	149.8(5)
O44i—U10—O53	146.2(5)	O32—V4—O31	78.8(6)
O19—U10—O74	83.1(6)	O36—V5—O37	110.4(7)
O20—U10—O74	96.0(5)	O36—V5—O35	105.8(6)
O46—U10—O74	139.7(5)	O37—V5—O35	85.8(6)
O55—U10—O74	75.0(5)	O36—V5—O39	109.9(7)
O44i—U10—O74	74.4(4)	O37—V5—O39	139.1(6)
O53—U10—O74	139.2(5)	O35—V5—O39	90.0(6)
O21—V1—O23	105.7(7)	O36—V5—O38	103.8(6)
O21—V1—O22	109.1(7)	O37—V5—O38	84.7(5)
O23—V1—O22	84.5(7)	O35—V5—O38	150.4(5)
O21—V1—O25	104.2(7)	O39—V5—O38	79.2(5)

(continuation)

O40—V6—O41	109.3(7)
O40—V6—O42	105.8(6)
O41—V6—O42	85.9(6)
O40—V6—O38	108.9(6)
O41—V6—O38	141.3(5)
O42—V6—O38	89.9(6)
O40—V6—O39	105.5(6)
O41—V6—O39	87.1(6)
O42—V6—O39	148.5(5)
O38—V6—O39	76.7(5)
O43—V7—O42	104.2(8)
O43—V7—O44	106.4(8)
O42—V7—O44	85.7(6)
O43—V7—O46i	105.4(7)
O42—V7—O46i	150.4(5)
O44—V7—O46i	86.6(6)
O43—V7—O45	112.2(7)
O42—V7—O45	89.6(6)
O44—V7—O45	141.0(5)
O46i—V7—O45	78.8(6)
O47—V8—O48	109.5(8)
O47—V8—O49	108.9(8)
O48—V8—O49	86.1(7)
O47—V8—O46	109.2(7)
O48—V8—O46	140.1(6)
O49—V8—O46	90.2(7)
O47—V8—O45i	101.5(7)
O48—V8—O45i	84.7(6)
O49—V8—O45i	149.6(6)
O46—V8—O45i	78.7(6)
O50—V9—O51	110.6(9)
O50—V9—O49	108.3(7)
O51—V9—O49	85.0(6)
O50—V9—O53	109.0(9)
O51—V9—O53	139.8(6)
O49—V9—O53	89.5(7)
O50—V9—O52	104.7(7)
O51—V9—O52	85.9(6)
O49—V9—O52	147.0(6)
O53—V9—O52	77.4(6)
O54—V10—O55	108.6(8)
O54—V10—O52	111.8(8)
O55—V10—O52	139.2(6)
O54—V10—O23	104.5(7)
O55—V10—O23	85.1(7)
O52—V10—O23	90.0(7)
O54—V10—O53	105.0(7)
O55—V10—O53	86.1(6)
O52—V10—O53	78.6(7)
O23—V10—O53	150.5(6)
V1—O22—U1	106.1(6)
V1—O22—U2	102.8(6)
U1—O22—U2	131.2(5)
V1—O23—V10	152.9(10)
V1—O23—U1	103.7(7)
V10—O23—U1	103.0(6)
V1—O24—V2	99.9(6)
V1—O24—U6	139.1(8)
V2—O24—U6	102.5(6)
V1—O25—V2	99.4(7)
V1—O25—U2	105.7(8)
V2—O25—U2	138.8(7)
V2—O27—U6	104.7(6)
V2—O27—U7	106.3(6)
U6—O27—U7	132.1(5)
V3—O28—V2	152.4(8)
V3—O28—U7	104.2(6)
V2—O28—U7	103.4(5)
V3—O30—U7	106.5(6)
V3—O30—U8	104.3(7)
U7—O30—U8	131.0(5)
V3—O31—V4	101.6(6)
V3—O31—U2	138.7(6)
V4—O31—U2	104.3(6)
V4—O32—V3	101.1(5)
V4—O32—U8	137.3(7)
V3—O32—U8	102.3(6)
V4—O34—U3	107.5(5)
V4—O34—U2	105.5(6)
U3—O34—U2	131.9(5)
V5—O35—V4	151.8(8)
V5—O35—U3	105.2(6)
V4—O35—U3	102.6(5)
V5—O37—U4	106.5(6)
V5—O37—U3	105.1(6)
U4—O37—U3	133.1(5)
V6—O38—V5	101.8(6)
V6—O38—U4	138.3(6)
V5—O38—U4	103.0(5)
V5—O39—V6	102.2(6)
V5—O39—U8	141.1(6)
V6—O39—U8	100.7(6)

(continuation)

V6—O41—U8	105.0(5)	U4i—O48—U5	131.5(5)
V6—O41—U9	106.5(6)	V8—O49—V9	153.0(9)
U8—O41—U9	131.0(5)	V8—O49—U5	103.7(6)
V7—O42—V6	153.6(8)	V9—O49—U5	103.3(7)
V7—O42—U9	103.5(5)	V9—O51—U5	106.0(6)
V6—O42—U9	102.8(6)	V9—O51—U6	104.5(6)
V7—O44—U9	105.8(6)	U5—O51—U6	132.4(6)
V7—O44—U10i	103.7(7)	V10—O52—V9	102.1(7)
U9—O44—U10i	133.7(5)	V10—O52—U6	140.0(7)
V8i—O45—V7	100.4(6)	V9—O52—U6	102.1(6)
V8i—O45—U4	103.5(6)	V9—O53—V10	101.7(7)
V7—O45—U4	138.4(6)	V9—O53—U10	137.9(7)
V7i—O46—V8	102.0(6)	V10—O53—U10	102.1(7)
V7i—O46—U10	103.0(6)	V10—O55—U10	106.3(7)
V8—O46—U10	137.8(6)	V10—O55—U1	107.5(6)
V8—O48—U4i	106.5(7)	U10—O55—U1	130.0(6)
V8—O48—U5	106.4(6)		

Symmetry code: (i) $-x+1, -y+1, -z+1$.

Table S9. Selected bond distances (Å) for *(EMIm)$_8$[(UO$_2$)$_2$(V$_{16}$O$_{46}$)]·4H$_2$O* (**2**).

U1—O2	1.807(7)	V4—O15	1.723(7)
U1—O1	1.815(7)	V4—O10	1.873(6)
U1—O25i	2.304(8)	V4—O16	1.891(7)
U1—O12	2.343(7)	V4—O13	1.989(7)
U1—O4	2.359(6)	V5—O17	1.633(7)
U1—O18	2.370(7)	V5—O18	1.700(7)
U1—O23i	2.368(7)	V5—O19i	1.924(7)
V1—O3	1.613(7)	V5—O13	1.934(7)
V1—O4	1.681(7)	V5—O16	2.014(7)
V1—O5	1.926(7)	V6—O20	1.604(7)
V1—O7	1.940(7)	V6—O21	1.703(7)
V1—O6	1.992(7)	V6—O5	1.881(6)
V2—O8	1.600(7)	V6—O16i	1.919(7)
V2—O9	1.716(7)	V6—O19	2.023(7)
V2—O6	1.886(7)	V7—O22	1.627(7)
V2—O10	1.931(7)	V7—O23	1.693(7)
V2—O7	1.988(7)	V7—O6	1.931(7)
V3—O11	1.617(8)	V7—O19	1.931(7)
V3—O12	1.696(7)	V7—O5	1.977(7)
V3—O7	1.913(7)	V8—O24	1.598(7)
V3—O13	1.937(7)	V8—O25	1.637(8)
V3—O10	2.020(7)	V8—O15	1.932(7)
V4—O14	1.605(7)	V8—O21i	1.963(7)

(continuation)

V8—O9	1.967(7)	V8A—O21i	1.612(9)
V8A—O25	1.061(10)	V8A—O24	2.124(9)

Symmetry code: (i) -x+1/2,-y+1/2,-z

Table S10. Selected angles (°) for *(EMIm)$_8$[(UO$_2$)$_2$(V$_{16}$O$_{46}$)]·4H$_2$O* (**2**).

O2—U1—O1	177.0(3)	O9—V2—O7	149.3(3)
O2—U1—O25i	92.8(3)	O6—V2—O7	76.7(3)
O1—U1—O25i	90.2(3)	O10—V2—O7	75.4(3)
O2—U1—O12	91.7(3)	O11—V3—O12	105.2(4)
O1—U1—O12	86.2(3)	O11—V3—O7	107.5(3)
O25i—U1—O12	143.6(2)	O12—V3—O7	94.9(3)
O2—U1—O4	91.9(3)	O11—V3—O13	107.3(3)
O1—U1—O4	89.6(3)	O12—V3—O13	96.7(3)
O25i—U1—O4	72.3(2)	O7—V3—O13	138.7(3)
O12—U1—O4	71.4(2)	O11—V3—O10	102.6(4)
O2—U1—O18	92.1(3)	O12—V3—O10	152.2(3)
O1—U1—O18	85.1(3)	O7—V3—O10	75.1(3)
O25i—U1—O18	144.4(3)	O13—V3—O10	76.3(3)
O12—U1—O18	71.4(2)	O14—V4—O15	103.8(4)
O4—U1—O18	142.7(2)	O14—V4—O10	111.5(3)
O2—U1—O23i	90.7(3)	O15—V4—O10	93.3(3)
O1—U1—O23i	89.5(3)	O14—V4—O16	110.1(3)
O25i—U1—O23i	74.4(3)	O15—V4—O16	92.2(3)
O12—U1—O23i	141.7(2)	O10—V4—O16	135.3(3)
O4—U1—O23i	146.7(2)	O14—V4—O13	102.1(4)
O18—U1—O23i	70.3(2)	O15—V4—O13	154.1(3)
O3—V1—O4	106.4(3)	O10—V4—O13	78.5(3)
O3—V1—O5	102.5(3)	O16—V4—O13	77.6(3)
O4—V1—O5	98.9(3)	O17—V5—O18	106.3(4)
O3—V1—O7	101.6(3)	O17—V5—O19i	107.3(3)
O4—V1—O7	94.2(3)	O18—V5—O19i	94.2(3)
O5—V1—O7	148.0(3)	O17—V5—O13	107.5(3)
O3—V1—O6	116.7(3)	O18—V5—O13	96.4(3)
O4—V1—O6	136.8(3)	O19i—V5—O13	138.9(3)
O5—V1—O6	75.1(3)	O17—V5—O16	102.1(3)
O7—V1—O6	75.4(3)	O18—V5—O16	151.6(3)
O8—V2—O9	105.3(4)	O19i—V5—O16	76.0(3)
O8—V2—O6	105.9(3)	O13—V5—O16	76.0(3)
O9—V2—O6	98.6(3)	O20—V6—O21	105.7(4)
O8—V2—O10	106.6(3)	O20—V6—O5	106.1(3)
O9—V2—O10	92.2(3)	O21—V6—O5	98.9(3)
O6—V2—O10	141.5(3)	O20—V6—O16i	105.4(3)
O8—V2—O7	105.1(3)	O21—V6—O16i	93.3(3)

(continuation)

O5—V6—O16i	141.5(3)	V6—O5—V7	106.1(3)
O20—V6—O19	103.5(3)	V1—O5—V7	104.6(3)
O21—V6—O19	150.7(3)	V2—O6—V7	151.0(4)
O5—V6—O19	75.7(3)	V2—O6—V1	104.9(3)
O16i—V6—O19	75.9(3)	V7—O6—V1	103.9(3)
O22—V7—O23	107.0(4)	V3—O7—V1	139.1(4)
O22—V7—O6	101.2(3)	V3—O7—V2	105.6(3)
O23—V7—O6	98.1(3)	V1—O7—V2	103.0(3)
O22—V7—O19	102.0(3)	V2—O9—V8	134.9(4)
O23—V7—O19	95.5(3)	V4—O10—V2	136.5(4)
O6—V7—O19	148.3(3)	V4—O10—V3	103.2(3)
O22—V7—O5	113.7(3)	V2—O10—V3	103.7(3)
O23—V7—O5	139.3(3)	V3—O12—U1	115.5(3)
O6—V7—O5	75.3(3)	V5—O13—V3	133.0(4)
O19—V7—O5	75.7(3)	V5—O13—V4	102.9(3)
O24—V8—O25	109.5(4)	V3—O13—V4	102.0(3)
O24—V8—O15	108.2(4)	V4—O15—V8	128.1(3)
O25—V8—O15	142.3(3)	V4—O16—V6i	134.4(4)
O24—V8—O21i	102.6(3)	V4—O16—V5	103.5(3)
O25—V8—O21i	92.4(3)	V6i—O16—V5	104.1(3)
O15—V8—O21i	79.0(3)	V5—O18—U1	115.6(3)
O24—V8—O9	103.4(3)	V5i—O19—V7	138.1(4)
O25—V8—O9	90.7(3)	V5i—O19—V6	103.6(3)
O15—V8—O9	81.0(3)	V7—O19—V6	102.5(3)
O21i—V8—O9	151.1(3)	V6—O21—V8i	136.7(4)
V1—O4—U1	130.9(3)	V7—O23—U1i	127.0(4)
V6—O5—V1	148.6(4)	V8—O25—U1i	145.6(4)

Symmetry code: (i) -x+1/2,-y+1/2,-z

References

1. Brese N.E., O'Keefee M. *Acta Crystallogr.*, **1991**, *B47*, 192-197.
2. Burns P.C., Ewing R.C., Hawthorne F.C. *The Canadian Mineralogist*, **1997**, *35*, 1551-1570.
3. Sheldrick, G. M. *SHELXTL*; Bruker AXS, Inc.: Madison, WI, **2008**.
4. Sheldrick, G. M. *SADABS*-Bruker AXS Area Detector Scaling and Adsorption, version 2008/1; University of Göttingen: Germany, **2008**.
5. Spek A.L. PLATON; J. Appl. Crystallogr., **2003**, 36, 7-13.